From bloodjournal.hematologylibrary.org at Hirosaki University on January 30, 2013. For personal use only.

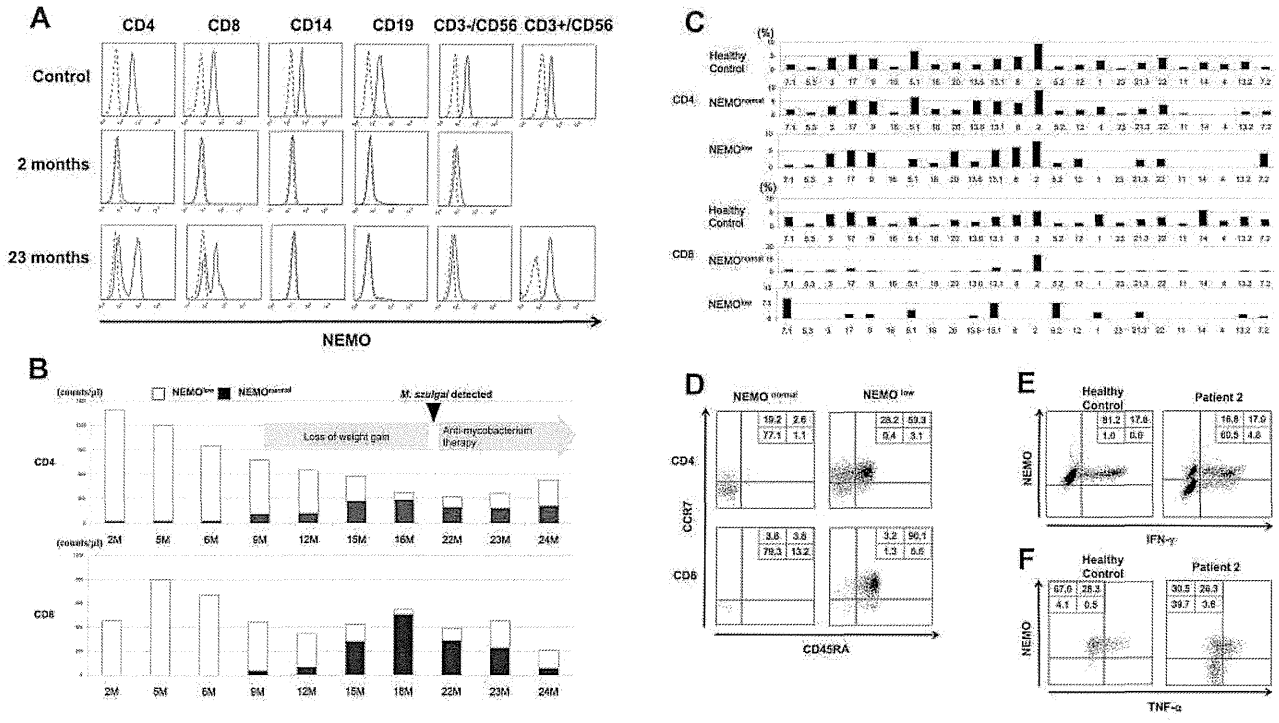

Figure 1. Identification and characterization of *NEMO* revertant T cells in patient 2. (A) Intracellular expression of NEMO in various PBMC lineages from a healthy adult control and patient 2 were evaluated by flow cytometry. For the patient, results of the analyses performed at 2 months and 23 months are shown. Solid lines indicate staining with the anti-NEMO mAb, and dotted lines indicate the isotype control. (B) Time-course variations in the absolute count of $NEMO^{normal}$ and $NEMO^{low}$ T cells in patient 2. M indicates age in months. (C) TCR-Vβ repertoire analysis of the patient's $CD4^+$ and $CD8^+$ T cells. PBMCs from the patient and a healthy adult control were stained for the TCR-Vβ panel, CD4, CD8, and NEMO, and analyzed by flow cytometry. (D) Phenotype analysis of T cells in patient 2. PBMCs from the patient and a control were stained for the expression of NEMO, CCR7, CD45RA, and CD4 or CD8. Data shown were gated on $NEMO^{normal}$ or $NEMO^{low}$ $CD4^+$ or $CD8^+$ cells. (E-F) Cytokine production from $NEMO^{normal}$ and $NEMO^{low}$ T cells. PBMCs from the patient and a control were stimulated with PMA and ionomycin for 6 hours and stained for intracellular (E) IFN-γ or (F) TNF-α along with NEMO. Cells shown are gated on the $CD3^+$ population.

because of X-chromosome inactivation. This analysis assumes that the percentage of cDNA for wild-type *NEMO* reflects the percentage of cells expressing wild-type NEMO. A high proportion of wild-type *NEMO* cDNA was observed in T cells from the mothers of patients 1/2, 3, 8, and 10, although wild-type *NEMO* cDNA was not predominant in T cells from the mother of patient 4 (Table 5).

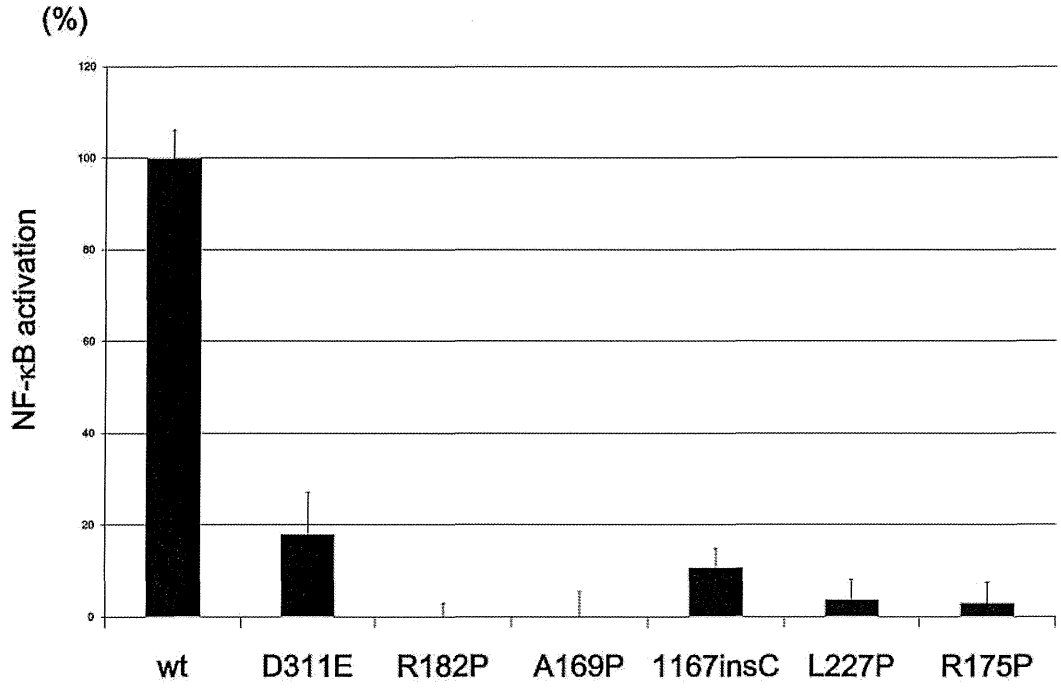

Figure 2. NF-κB transactivation by NEMO mutants from the XL-EDA-ID patients. NF-κB transactivation induced by NEMO mutants in the XL-EDA-ID patients. Mock vectors and wild-type (wt) NEMO were used as controls. The NF-κB activation index of NEMO variants were calculated as (NF-κB activation by each NEMO variant − NF-κB activation of the mock vector)/(NF-κB activation by wild-type NEMO − NF-κB activation of the mock vector). The data shown are the mean ± SD of triplicate wells and are representative of 3 independent experiments with similar results.

From bloodjournal.hematologylibrary.org at Hirosaki University on January 30, 2013. For personal use only.

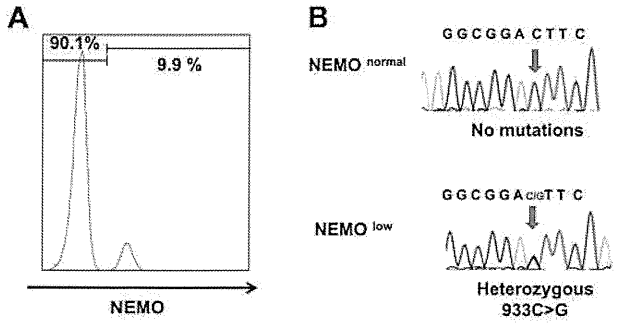

Figure 3. *NEMO* revertant T cells in patient 3. (A) Intracellular expression of NEMO in CD8+ cells from patient 3. (B) Sequencing chromatograms of DNA from NEMO^{normal} or NEMO^{low} CD8+ cells of patient 3. Arrows indicate the mutated base position at c. 931.

Similarly, there was an apparent high proportion of wild-type *NEMO* cDNA in monocytes and B cells from the mothers of patients 1/2, 8, and 10 (Table 5). These findings suggested a general selective advantage of NEMO^{normal} cells over NEMO^{low} cells in vivo, especially in T cells.

Proliferation capacity of NEMO^{normal} and NEMO^{low} T cells

T-cell proliferation stimulated by mitogens such as PHA is usually not reduced in XL-EDA-ID patients. However, the emergence of NEMO^{normal} cells coincided with a reduction in mitogen-induced proliferation in patient 2. To further determine the effect of NEMO^{normal} cells on mitogen-induced proliferation of peripheral T cells, the proportions of T cells carrying the wild-type and mutant were examined before and after PHA stimulation in XL-EDA-ID patients and their mothers (Table 6). In patients 2, 4, and 8, the percentage of the NEMO^{normal} cells decreased after PHA stimulation, while NEMO^{normal} cells prevailed in patient 9. In the mothers of patient 4 and 10, the percentage of NEMO^{normal} cells increased after PHA stimulation, while the percentage of the NEMO^{normal} cells decreased in the mother of patient 3. These results indicated that the NEMO mutation does not directly affect the mitogen-induced proliferation capacity of T cells and factors other than the *NEMO* genotype determine the proliferation capacity of NEMO^{normal} and NEMO^{low} T cells.

Discussion

Somatic reversion mosaicism has been described in several disorders affecting the hematopoietic system, the liver, and the skin.[23,26] Reports of somatic reversion cases have been particularly abundant in patients with immunodeficiency diseases, including Wiskott-Aldrich syndrome (WAS)[27] and SCID, which occur because of mutations in the interleukin receptor common γ chain,[28] CD3ζ,[29] *RAG-1*[30], and *ADA* genes.[31] Patients with somatic reversion mosaicism may present with significantly milder clinical phenotypes compared with nonrevertant patients with the same germline mutation, although this is not always the case.[26] One common feature in most cases where the somatic reversion mosaicism has been observed is a strong in vivo selective advantage of the revertant cells that express the wild-type gene product. One of the most intensively investigated diseases associated with somatic reversion mosaicism is WAS.[32-34] A report showed that up to 11% of WAS patients have presented with somatic reversion mosaicism.[33]

In our investigation, 9 of 10 XL-EDA-ID patients presented with somatic mosaicism. Two of the 9 were cases of reversion from a duplication mutation, while the others exhibited true back-reversion from a substitution or insertion mutation. This finding calls for caution when diagnosing XL-EDA-ID patients. Because the existence of a *NEMO* pseudogene makes it difficult to perform genetic analysis using genomic DNA, diagnosis of the disease is often confirmed by sequencing analysis of *NEMO* cDNA, and the presence of somatic mosaicism can cause misdiagnosis of XL-EDA-ID patients either when NEMO^{normal} cells make up the majority of the patients' PBMCs or when the cDNA of the mutated *NEMO* gene cannot be amplified by PCR.[17] In fact, mutated *NEMO* cDNA could not be amplified from the PBMCs of patient 2 even when NEMO^{normal} cells were absent (during early infancy), and only wild-type *NEMO* cDNA was amplified after the appearance of NEMO^{normal} cells (data not shown), probably because of the instability of the mutated *NEMO* mRNA. Flow cytometric analysis of intracellular NEMO protein is of help in identifying the NEMO^{low} cells in some patients, but the technique is not applicable when the *NEMO* mutation does not cause reduced expression of NEMO protein. Thus, some cases of XL-EDA-ID patients with reversion may be difficult to diagnose.

The high frequency of somatic mosaicism observed in XL-EDA-ID patients indicates a strong in vivo selective advantage for NEMO^{normal} cells, which express the wild-type gene product. Patient 2 presented with a high mutant T-cell count at birth that gradually decreased over time (Figure 1B). This finding indicates that wild-type NEMO expression is critical for the survival of certain cell lineages, including T cells, after birth. On the other hand, no NEMO^{normal} monocytes and very few NEMO^{normal} B cells were detected in the recruited XL-EDA-ID patients (Table 4). This specific feature is similar to other somatic reversion mosaicism seen in primary immunodeficiency patients[26] and indicates that the expression of NEMO is less critical for the survival of monocytes or B cells compared with that of T cells. There is also an apparent

Table 4. Analysis of *NEMO* gene mosaicism in various cell lineages for each patient

Patient	Mutation	Age at analysis	CD4, % (proportion)	CD8, % (proportion)	CD14, % (proportion)	CD19, % (proportion)
1	Duplication	2 y	90	100	0	4.0
2	Duplication	15 mo	45	66	0	4.0
3	D311E	3 y	2.4	9.9	0	1.2
4	A169P	12 y	0 (0/19)	24 (9/37)	0 (0/19)	0 (0/47)
5	L227P	3 y	0 (0/25)	0 (0/35)	0 (0/30)	0 (0/25)
6	R182P	4 y	18 (5/28)	17 (9/52)	0 (0/27)	0 (0/33)
7	R175P	6 y	0.4 (1/25)	39 (11/28)	0 (0/28)	0 (0/25)
8	Q348X	8 y	38 (6/16)	47 (9/19)	0 (0/33)	0 (0/25)
9	R175P	15 y	30 (9/30)	36 (12/33)	0 (0/23)	0 (0/14)
10	1167 ins C	9 mo		PBMC 9.3 (4/43)		

For patients 1 to 3, data represent the percentages of NEMO^{normal} cells in each lineage, as assessed by flow cytometry. For patients 4 to 10, the ratio indicates the number of wild-type NEMO clones in various cell lineages as compared with the total number of clones analyzed, based on subcloning and sequencing analysis.

From bloodjournal.hematologylibrary.org at Hirosaki University on January 30, 2013. For personal use only.

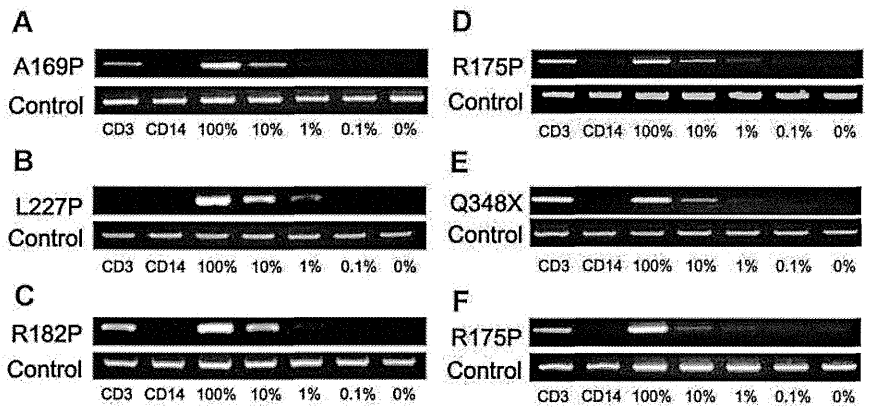

Figure 4. NEMO reversion selectively occurs in T cells of XL-EDA-ID patients. Allele-specific PCR for *NEMO* on CD3+ or CD14+ cells from (A) patient 4, (B) patient 5, (C) patient 6, (D) patient 7, (E) patient 8, and (F) patient 9. Numbers below each figure indicate the percentages of wild-type NEMO cDNA mixed with each mutant. Primers used in each PCR are shown on the left.

concordance between the degree of the disruption of *NEMO* gene and the proportion of reverted NEMO^{normal} cells compared with NEMO^{low} cells. The high proportion of reverted T cells seen in patients 1 and 2 as well as in patient 8 was associated with a highly disruptive mutation of the *NEMO* gene (ie, a duplication mutation in patients 1 and 2, and a truncation mutation in patient 8). In addition, the highly selective X-chromosome inactivation observed in the mothers of XL-EDA-ID patients indicated a strong selective advantage for NEMO^{normal} cells over NEMO^{low} cells. It is also noteworthy that reverted T cells were not detected in patient 5, who carried an L227P mutation that was not localized to either of the functional domains in the NEMO protein. Other reported cases with the same mutation presented with polysaccharide-specific humoral immunodeficiency and autoinflammatory diseases, but were spared complications such as cellular immunodeficiency and susceptibility to *Mycobacterium* (similar to patient 5).[4,8] This may reflect the fact that the L227P mutation in NEMO has less influence on T-cell growth than NEMO mutations that occur in functional domains, and suggests that reversion of the mutation has little impact on T-cell survival. Although the number of cases in our study is limited, it appears that the more disruptive NEMO mutations favor the survival of NEMO^{normal} cells after reversion and X-chromosome inactivation.

Regarding the gradual decline in the number of NEMO-deficient T cells, one candidate trigger could be infection. Because the dominance of the memory phenotype and the skewed TCR repertoire among CD8+ T cells in NEMO^{normal} cells were observed in both patients 1 and 2 (Figure 1C and Mizukami et al[18]), continuous infection of pyogenic bacteria in patient 1 and *M szulgai* in patient 2 could be a reason for the emergence of NEMO^{normal} cells and the elimination of NEMO^{low} cells. The decrease in NEMO^{normal} cells and restoration of NEMO^{low} cells after anti-mycobacterial therapy in patient 2 support this hypothesis. In the case of patient 1, the predominance of NEMO^{normal} T cells with an effector/memory phenotype at diagnosis (Table 4 and Mizukami et al[18]) is likely to be the result of chronic infection, and it is possible that NEMO^{low} cells were predominant during his early infancy. Because some reports have indicated that TNF-α–induced programmed cell death of several cell types, including a human T-cell line, was enhanced by hypomorphic *NEMO* mutations,[12,35] and considering our finding that the levels of TNF-α expressed in revertant T cells were similar to levels in healthy control T cells in vitro (Figure 1F), TNF-α produced from these cells in response to infection could be involved in mutant T-cell elimination.

Unexpectedly, T-cell proliferation in patient 2 was equivalent to that of normal controls at the age of 2 months and was reduced after NEMO^{normal} T cells increased (Figure 1B; Table 3). This finding indicates that the NEMO^{low} T cells did not have intrinsically impaired mitogen-induced proliferation. One reasonable explanation for the reduced proliferation observed after the increase in NEMO^{normal} T cells is a reduction in the absolute number of T cells (naive T cells in particular), probably because of the infection.

Table 5. Expression of mutant NEMO in various cell lineages for the mother of each XL-EDA-ID patient

Sample	Mutation	Analysis	Subtype	Mutant type, % (proportion)
Mother of patients 1 and 2	Duplication	FACS	CD3	0
			CD14	0
			CD19	0
Mother of patient 3	D311E	FACS	CD3	13
			CD3−	54
		Subcloning	CD3	22 (6/27)
			CD3−	55 (12/22)
Mother of patient 4	A169P	Subcloning	CD3	52 (11/21)
			CD14	58 (11/19)
			CD19	42 (5/12)
Mother of patient 8	Q348X	Subcloning	CD3	0 (0/26)
			CD14	17 (3/18)
			CD19	0 (0/18)
Mother of patient 10	1167insC	Subcloning	CD3	18 (7/39)
			CD14	12 (5/43)
			CD19	27 (12/44)

Data are shown as either the percentages of NEMO^{normal} cells, as assessed by flow cytometry, or as the ratio of clones containing wild-type NEMO to the total number of clones, as analyzed by subcloning and sequencing analysis.

From bloodjournal.hematologylibrary.org at Hirosaki University on January 30, 2013. For personal use only.

Table 6. Expression of mutant NEMO in CD3-positive cells and PHA blasts

Sample	Mutations	Analysis	Subtype	Mutant type, % (proportion)
Mother of patient 3	D311E	FACS	CD3	13
			PHA blast	47
		Subcloning	CD3	22 (6/27)
			PHA blast	48 (11/23)
Mother of patient 4	A169P	Subcloning	CD3	52 (11/21)
			PHA blast	18 (9/49)
Mother of patient 8	Q348X	Subcloning	CD3	0 (0/26)
			PHA blast	0 (0/21)
Mother of patient 10	1167insC	Subcloning	CD3	18 (7/39)
			PHA blast	9 (4/43)
Patient 2	Duplication	FACS	CD3	73
			PHA blast	93
Patient 4	A169P	Subcloning	CD3	79 (19/24)
			PHA blast	100 (37/37)
Patient 8	Q348X	Subcloning	CD3	56 (18/32)
			PHA blast	100 (16/16)
Patient 9	R175P	Subcloning	CD3	87 (34/39)
			PHA blast	0 (0/28)

PHA blasts were obtained by incubating PBMCs with PHA and soluble IL-2 for 7 days. Data are shown as either the percentages of $NEMO^{normal}$ cells, as assessed by flow cytometry, or as the ratio of clones containing wild-type NEMO to the total number of clones, as analyzed by subcloning and sequencing analysis.

Therefore, to identify other mechanisms underlying reduced T-cell proliferation, the impact of *NEMO* mutation on PHA-induced T-cell proliferation was indirectly examined in vitro by comparing the response of $NEMO^{normal}$ and $NEMO^{low}$ cells derived from XL-EDA-ID patients and their mothers. After PHA stimulation and proliferation, the proportion of $NEMO^{low}$ T cells increased in patients 2, 4, and 8, while the opposite result was observed in patient 9 and in the mother of patient 4 (Table 6). Although the precise mechanism is unclear, a reduction in the proportion of $NEMO^{normal}$ cells after PHA stimulation would reflect the lower proliferative capacity of $NEMO^{normal}$ cells compared with that of $NEMO^{low}$ cells, which may be another explanation for the reduced T-cell proliferation observed in patient 2 at 23 months of age when $NEMO^{normal}$ T cells were dominant. In the reports on reversion mosaicism of *IL2RG* gene mutations,[28,36] the restoration of T-cell function and clinical symptoms varied among patients. Therefore, other factors besides the genotype of the mutations, such as the developmental stage where reversion occurred and the frequency of reversion, affect the clinical impact of somatic mosaicism of *NEMO* gene mutations.

In this study, the effect of somatic mosaicism of the *NEMO* gene on clinical phenotype could not be fully evaluated. However, cytokines produced by revertant T cells could influence the development of clinical symptoms of XL-EDA-ID, such as inflammatory bowel disease. In a mouse model, intestinal epithelial cell-specific inhibition of NF-κB through the conditional ablation of NEMO resulted in the development of chronic bowel inflammation sensitized intestinal epithelial cells to TNF-α–induced apoptosis.[37] In this model, the first phase of intestinal inflammation was initiated by epithelial cell death and was followed by a second phase of TNF-α–induced intestinal inflammation, the latter being dependent on T cells. Another report showed that HSCT in XL-EDA-ID patients exacerbated the patients' inflammatory bowel disease.[38] Indeed, in patient 4, the percentage of reverted T cells was reduced after repeated administrations of anti-TNFα blocking Ab, and the symptoms of inflammatory bowel disease improved.[18] Considering this evidence, somatic mosaicism in T cells might be an important factor leading to inflammatory disease in XL-EDA-ID patients with defective NF-κB activation. However, our study did not show a tight association between inflammatory bowel disease and somatic mosaicism, and further investigation is needed to determine whether the $NEMO^{normal}$ T cells play a role in inflammatory processes in XL-EDA-ID.

In conclusion, this study has identified a high frequency of somatic mosaicism in XL-EDA-ID patients, particularly in T cells, and has revealed important insights into human T-cell immunobiology in XL-EDA-ID. Although we could not demonstrate the clinical impact of somatic mosaicism in XL-EDA-ID patients, our findings suggest that care is required when making molecular diagnoses of XL-EDA-ID, and might shed light on the mechanisms underlying the variability in the clinical manifestation of XL-ED-ID and facilitate the search for appropriate treatments.

Acknowledgments

The authors are grateful to all the XL-EDA-ID patients and their families for their participation. They also thank Shoji Yamaoka (Department of Molecular Virology, Graduate School of Medicine, Tokyo Medical and Dental University, Tokyo, Japan) for kindly providing NEMO-null rat fibroblast cells, and Takeda Pharmaceutical Company Limited for kindly providing the recombinant human IL-2.

This work was supported by grants from the Japanese Ministry of Education, Culture, Sports, Science, and Technology, and by grants from the Japanese Ministry of Health, Labor and Welfare.

Authorship

Contribution: Tomoki Kawai wrote the manuscript and performed research; R.N., T.Y., T.N., and T.H. edited the manuscript and supervised this work; K.I., Y.M., N.T., H.S., M.S., and Y.T. cultured cells; and T. Mizukami, H.N., Y.K., A.Y., T. Murata, S.S., E.I., H.A., Toshinao Kawai, C.I., S.O., and M.K. treated patients and analyzed data.

Conflict-of-interest disclosure: The authors declare no competing financial interests.

Correspondence: Ryuta Nishikomori, MD, PhD, Department of Pediatrics, Kyoto University Graduate School of Medicine, 54 Kawahara-cho, Shogoin, Sakyo-ku, Kyoto 606-8507, Japan; e-mail: rnishiko@kuhp.kyoto-u.ac.jp.

From bloodjournal.hematologylibrary.org at Hirosaki University on January 30, 2013. For personal use only.

References

1. Pinheiro M, Freire-Maia N. Ectodermal dysplasias: a clinical classification and a causal review. *Am J Med Genet.* 1994;53(2):153-162.
2. Abinun M, Spickett G, Appleton AL, Flood T, Cant AJ. Anhidrotic ectodermal dysplasia associated with specific antibody deficiency. *Eur J Pediatr.* 1996;155(2):146-147.
3. Sitton JE, Reimund EL. Extramedullary hematopoiesis of the cranial dura and anhidrotic ectodermal dysplasia. *Neuropediatrics.* 1992;23(2):108-110.
4. Schweizer P, Kalhoff H, Horneff G, Wahn V, Diekmann L. [Polysaccharide specific humoral immunodeficiency in ectodermal dysplasia. Case report of a boy with two affected brothers]. *Klin Padiatr.* 1999;211(6):459-461.
5. Abinun M. Ectodermal dysplasia and immunodeficiency. *Arch Dis Child.* 1995;73(2):185.
6. Zonana J, Elder ME, Schneider LC, et al. A novel X-linked disorder of immune deficiency and hypohidrotic ectodermal dysplasia is allelic to incontinentia pigmenti and due to mutations in IKK-gamma (NEMO). *Am J Hum Genet.* 2000;67(6):1555-1562.
7. Courtois G, Smahi A, Israel A. NEMO/IKK gamma: linking NF-kappa B to human disease. *Trends Mol Med.* 2001;7(10):427-430.
8. Doffinger R, Smahi A, Bessia C, et al. X-linked anhidrotic ectodermal dysplasia with immunodeficiency is caused by impaired NF-kappaB signaling. *Nat Genet.* 2001;27(3):277-285.
9. Rothwarf DM, Zandi E, Natoli G, Karin M. IKK-gamma is an essential regulatory subunit of the IkappaB kinase complex. *Nature.* 1998;395(6699):297-300.
10. Yamaoka S, Courtois G, Bessia C, et al. Complementation cloning of NEMO, a component of the IkappaB kinase complex essential for NF-kappaB activation. *Cell.* 1998;93(7):1231-1240.
11. Smahi A, Courtois G, Vabres P, et al. Genomic rearrangement in NEMO impairs NF-kappaB activation and is a cause of incontinentia pigmenti. The International Incontinentia Pigmenti (IP) Consortium. *Nature.* 2000;405(6785):466-472.
12. Hanson EP, Monaco-Shawver L, Solt LA, et al. Hypomorphic nuclear factor-kappaB essential modulator mutation database and reconstitution system identifies phenotypic and immunologic diversity. *J Allergy Clin Immunol.* 2008;122(6):1169-1177.
13. Orange JS, Jain A, Ballas ZK, Schneider LC, Geha RS, Bonilla FA. The presentation and natural history of immunodeficiency caused by nuclear factor kappaB essential modulator mutation. *J Allergy Clin Immunol.* 2004;113(4):725-733.
14. Jain A, Ma CA, Liu S, Brown M, Cohen J, Strober W. Specific missense mutations in NEMO result in hyper-IgM syndrome with hypohydrotic ectodermal dysplasia. *Nat Immunol.* 2001;2(3):223-228.
15. Orange JS, Brodeur SR, Jain A, et al. Deficient natural killer cell cytotoxicity in patients with IKK-gamma/NEMO mutations. *J Clin Invest.* 2002;109(11):1501-1509.
16. Sebban H, Courtois G. NF-kappaB and inflammation in genetic disease. *Biochem Pharmacol.* 2006;72(9):1153-1160.
17. Nishikomori R, Akutagawa H, Maruyama K, et al. X-linked ectodermal dysplasia and immunodeficiency caused by reversion mosaicism of NEMO reveals a critical role for NEMO in human T-cell development and/or survival. *Blood.* 2004;103(12):4565-4572.
18. Mizukami T, Obara M, Nishikomori R, et al. Successful treatment with infliximab for inflammatory colitis in a patient with X-linked anhidrotic ectodermal dysplasia with immunodeficiency. *J Clin Immunol.* 2012;32(1):39-49.
19. Imamura M, Kawai T, Okada S, et al. Disseminated BCG infection mimicking metastatic nasopharyngeal carcinoma in an immunodeficient child with a novel hypomorphic NEMO mutation. *J Clin Immunol.* 2011;31(5):802-810.
20. Tono C, Takahashi Y, Terui K, et al. Correction of immunodeficiency associated with NEMO mutation by umbilical cord blood transplantation using a reduced-intensity conditioning regimen. *Bone Marrow Transplant.* 2007;39(12):801-804.
21. Saito M, Nishikomori R, Kambe N, et al. Disease-associated CIAS1 mutations induce monocyte death, revealing low-level mosaicism in mutation-negative cryopyrin-associated periodic syndrome patients. *Blood.* 2008;111(4):2132-2141.
22. Yang TP, Stout JT, Konecki DS, Patel PI, Alford RL, Caskey CT. Spontaneous reversion of novel Lesch-Nyhan mutation by HPRT gene rearrangement. *Somat Cell Mol Genet.* 1988;14(3):293-303.
23. Zhang LH, Jenssen D. Reversion of the hprt mutant clone SP5 by intrachromosomal recombination. *Carcinogenesis.* 1992;13(4):609-615.
24. Monnat RJ Jr, Chiaverotti TA, Hackmann AF, Maresh GA. Molecular structure and genetic stability of human hypoxanthine phosphoribosyltransferase (HPRT) gene duplications. *Genomics.* 1992;13(3):788-796.
25. Rautenstrauss B, Liehr T, Fuchs C, et al. Mosaicism for Charcot-Marie-Tooth disease type 1A: onset in childhood suggests somatic reversion in early developmental stages. *Int J Mol Med.* 1998;1(2):333-337.
26. Wada T, Candotti F. Somatic mosaicism in primary immune deficiencies. *Curr Opin Allergy Clin Immunol.* 2008;8(6):510-514.
27. Ariga T, Kondoh T, Yamaguchi K, et al. Spontaneous in vivo reversion of an inherited mutation in the Wiskott-Aldrich syndrome. *J Immunol.* 2001;166(8):5245-5249.
28. Stephan V, Wahn V, Le Deist F, et al. Atypical X-linked severe combined immunodeficiency due to possible spontaneous reversion of the genetic defect in T cells. *N Engl J Med.* 1996;335(21):1563-1567.
29. Rieux-Laucat F, Hivroz C, Lim A, et al. Inherited and somatic CD3zeta mutations in a patient with T-cell deficiency. *N Engl J Med.* 2006;354(18):1913-1921.
30. Wada T, Toma T, Okamoto H, et al. Oligoclonal expansion of T lymphocytes with multiple second-site mutations leads to Omenn syndrome in a patient with RAG1-deficient severe combined immunodeficiency. *Blood.* 2005;106(6):2099-2101.
31. Hirschhorn R. In vivo reversion to normal of inherited mutations in humans. *J Med Genet.* 2003;40(10):721-728.
32. Wada T, Schurman SH, Jagadeesh GJ, Garabedian EK, Nelson DL, Candotti F. Multiple patients with revertant mosaicism in a single Wiskott-Aldrich syndrome family. *Blood.* 2004;104(5):1270-1272.
33. Stewart DM, Candotti F, Nelson DL. The phenomenon of spontaneous genetic reversions in the Wiskott-Aldrich syndrome: a report of the workshop of the ESID Genetics Working Party at the XIIth Meeting of the European Society for Immunodeficiencies (ESID). Budapest, Hungary October 4-7, 2006. *J Clin Immunol.* 2007;27(6):634-639.
34. Davis BR, Yan Q, Bui JH, et al. Somatic mosaicism in the Wiskott-Aldrich syndrome: molecular and functional characterization of genotypic revertants. *Clin Immunol.* 2010;135(1):72-83.
35. Yamaoka S, Inoue H, Sakurai M, et al. Constitutive activation of NF-kappa B is essential for transformation of rat fibroblasts by the human T-cell leukemia virus type I Tax protein. *EMBO J.* 1996;15(4):873-887.
36. Speckmann C, Pannicke U, Wiech E, et al. Clinical and immunologic consequences of a somatic reversion in a patient with X-linked severe combined immunodeficiency. *Blood.* 2008;112(10):4090-4097.
37. Nenci A, Becker C, Wullaert A, et al. Epithelial NEMO links innate immunity to chronic intestinal inflammation. *Nature.* 2007;446(7135):557-561.
38. Fish JD, Duerst RE, Gelfand EW, Orange JS, Bunin N. Challenges in the use of allogeneic hematopoietic SCT for ectodermal dysplasia with immune deficiency. *Bone Marrow Transplant.* 2009;43(3):217-221.

From bloodjournal.hematologylibrary.org at Hirosaki University on January 30, 2013. For personal use only.

Frequent somatic mosaicism of *NEMO* in T cells of patients with X-linked anhidrotic ectodermal dysplasia with immunodeficiency

Tomoki Kawai,[1] Ryuta Nishikomori,[1] Kazushi Izawa,[1] Yuuki Murata,[1] Naoko Tanaka,[1] Hidemasa Sakai,[1] Megumu Saito,[2] Takahiro Yasumi,[1] Yuki Takaoka,[1] Tatsutoshi Nakahata,[2] Tomoyuki Mizukami,[3] Hiroyuki Nunoi,[3] Yuki Kiyohara,[4] Atsushi Yoden,[5] Takuji Murata,[5] Shinya Sasaki,[6] Etsuro Ito,[6] Hiroshi Akutagawa,[7] Toshinao Kawai,[8] Chihaya Imai,[9] Satoshi Okada,[10] Masao Kobayashi,[10] and Toshio Heike[1]

[1]Department of Pediatrics, Kyoto University Graduate School of Medicine, Kyoto, Japan; [2]Clinical Application Department, Center for iPS Cell Research and Application, Institute for Integrated Cell-Material Sciences, Kyoto University, Kyoto, Japan; [3]Division of Pediatrics, Department of Reproductive and Developmental Medicine, Faculty of Medicine, University of Miyazaki, Miyazaki, Japan; [4]Department of Pediatrics, Faculty of Medicine, Osaka University, Suita, Japan; [5]Department of Pediatrics, Osaka Medical College, Takatsuki, Japan; [6]Department of Pediatrics, Hirosaki University Graduate School of Medicine, Hirosaki, Japan; [7]Department of Pediatrics, Kishiwada City Hospital, Kishiwada, Japan; [8]Department of Human Genetics, National Center for Child Health and Development, Tokyo, Japan; [9]Department of Pediatrics, Niigata University, Niigata, Japan; and [10]Department of Pediatrics, Hiroshima University Graduate School of Biomedical Sciences, Hiroshima, Japan

Somatic mosaicism has been described in several primary immunodeficiency diseases and causes modified phenotypes in affected patients. X-linked anhidrotic ectodermal dysplasia with immunodeficiency (XL-EDA-ID) is caused by hypomorphic mutations in the *NF-κB essential modulator (NEMO)* gene and manifests clinically in various ways. We have previously reported a case of XL-EDA-ID with somatic mosaicism caused by a duplication mutation of the *NEMO* gene, but the frequency of somatic mosaicism of *NEMO* and its clinical impact on XL-EDA-ID is not fully understood. In this study, somatic mosaicism of *NEMO* was evaluated in XL-EDA-ID patients in Japan. Cells expressing wild-type NEMO, most of which were derived from the T-cell lineage, were detected in 9 of 10 XL-EDA-ID patients. These data indicate that the frequency of somatic mosaicism of *NEMO* is high in XL-ED-ID patients and that the presence of somatic mosaicism of *NEMO* could have an impact on the diagnosis and treatment of XL-ED-ID patients. (*Blood.* 2012;119(23):5458-5466)

Introduction

X-linked anhidrotic ectodermal dysplasia with immunodeficiency (XL-EDA-ID) is a disease with clinical features including hypohidrosis, delayed eruption of teeth, coarse hair, and immunodeficiency associated with frequent bacterial infections.[1-5] The gene responsible for XL-EDA-ID has been identified as *NF-κB essential modulator (NEMO)*.[6-8] NEMO is necessary for the function of IκB kinase, which phosphorylates and degrades IκB to activate NF-κB.[9-10] Defects in NEMO cause various abnormalities in signal transduction pathways involving NF-κB, and affect factors such as the IL-1 family protein receptors, the TLRs, VEGFR-3, receptor activator of nuclear factor κB (RANK), the ectodysplasin-A receptor, CD40, and the TNF receptor I.[7] Whereas a complete loss of NEMO function in humans is believed to cause embryonic lethality,[11] *NEMO* mutations in XL-EDA-ID patients are hypomorphic,[8] causing a partial loss of NEMO functions.

In XL-EDA-ID, NEMO defects lead to diverse immunologic features including susceptibility to pathogens, impaired Ab response to polysaccharides,[2,4,12] hypogammaglobulinemia,[13] hyper IgM syndrome,[14] and impaired NK-cell activity,[15] with a large degree of variability in phenotypes among the patients. For example, approximately one-tenth of XL-EDA-ID patients exhibit reduced mitogen-induced proliferation of T lymphocytes.[12] Moreover, one-fourth suffer from inflammatory disorders such as inflammatory bowel disease and rheumatoid arthritis,[12] although the inflammatory process usually relies on NF-κB activation.[16] One explanation for this clinical variability is that the XL-EDA-ID phenotype is *NEMO* genotype-specific. Although the XL-EDA-ID database reported by Hanson et al succeeds to some extent in linking the specific clinical features to *NEMO* genotype,[12] the penetrance of some clinical features is not high and the mechanism accounting for this variability is unknown.

Recently, we have reported a case of spontaneous reversion mosaicism of the *NEMO* gene in XL-EDA-ID, which showed an atypical phenotype involving decreased mitogen-induced T-cell proliferation along with decreased CD4 T cells (patient 1).[17] There have been no subsequent reports on somatic mosaicism in XL-EDA-ID, and its prevalence and impact on the clinical features of the disease is unknown. In this study, we describe the younger brother of patient 1, who suffered from XL-EDA-ID with the same mutation and somatic reversion mosaicism of *NEMO*. Patient 2 showed intriguing laboratory findings in that mitogen-induced T-cell proliferation varied in accordance with the rate of detected reversion in the peripheral blood. These 2 cases led us to perform a nationwide study of XL-EDA-ID patients in Japan that revealed a high incidence of somatic mosaicism of *NEMO*.

Submitted May 11, 2011; accepted April 8, 2012. Prepublished online as *Blood* First Edition paper, April 19, 2012; DOI 10.1182/blood-2011-05-354167.

The online version of this article contains a data supplement.

The publication costs of this article were defrayed in part by page charge payment. Therefore, and solely to indicate this fact, this article is hereby marked "advertisement" in accordance with 18 USC section 1734.

© 2012 by The American Society of Hematology

From bloodjournal.hematologylibrary.org at Hirosaki University on January 30, 2013. For personal use only.

Table 1. Clinical and genetic features of XL-EDA-ID patients

Patient	Mutation	Ectodermal dysplasia	Mitogen-induced proliferation	Infections	Complications	Therapy	Sex chromosome chimerism
1	Duplication	+	Reduced	Sepsis (S.P. and P.A.)	Chronic diarrhea	IVIG	100% XY
				Disseminated M.A.C.	Failure to thrive	RFP, CAM, AMK, EB	
				Skin abscess (S.A.)	Small intestinal stenosis	Rifabutin	
				Invasive *Aspergillus*	Lymphedema		
2	Duplication	+	Reduced	Sepsis (*E coli*)	Failure to thrive	IVIG, ST, EB, CAM	99.8% XY 0.2% X
				Disseminated M.S.		Rifabutin, SCT	
3	D311E	−	Normal	Disseminated B.C.G.		IVIG, INH	100% XY
				Sepsis (S.P.)		RFP, SCT	
4	A169P	+	Normal	Meningitis (S.P.)	IBD	IVIG, ST, PSL	99% XY
					Interstitial pneumonia	CyA, MTX, Infliximab	
					Rheumatoid arthritis		
5	L227P	+	Normal	Recurrent pneumonia	IBD	ST, mesalazine	Not done
				Pyogenic coxitis		Infliximab	
				Recurrent otitis media			
6	R182P	+	Not done	Recurrent otitis media	IBD	ST, mesalazine	99.8% XY 0.2% X
				UTI, Recurrent stomatitis			
				Subepidermal abscess			
7	R175P	+	Normal	Recurrent sepsis (S.P.)		IVIG	100% XY
8	Q348X	+	Normal	Disseminated B.C.G.	IBD	IVIG, ST	100% XY
9	R175P	+	Normal	Recurrent pneumonia	IBD	IVIG	100% XY
				Recurrent otitis media		5-aminosalicylic acid	
				Kaposi varicelliform eruption			
10	1167 ins C	+	Normal	Sepsis and Enteritis (E.A)	Failure to thrive	IVIG, SCT	Not done
				Sepsis (C.G.)	Pyloric stenosis, colon polyps		
				UTI (K.P.)			

S.P. indicates *Streptococcus pneumoniae*; P.A., *Pseudomonas aeruginosa*; IVIG, intravascular immunoglobulin infusion; M.A.C., *Mycobacterium avium* complex; S.A., *Staphylococcus aureus*; *E coli*, *Escherichia coli*; ST, trimethoprim-sulfamethoxazole; M.S., *Mycobacterium szulgai*; AMK, amikacin; EB, ethambutol; CAM, clarithromycin; SCT, stem cell transplantation; B.C.G., Bacille de Calmette et Guerin; INH, isoniazid; RFP, rifampicin; IBD, inflammatory bowel disease; PSL, prednisolone; CyA, cyclosporine A; MTX, methotrexate; UTI, urinary tract infection; E.A., *Enterobacter aerogenes*; C.G., *Candida glabrata*; and K.P., *Klebsiella* pneumonia.

Methods

Informed consent

Informed consent was obtained from the patients and their families following the Declaration of Helsinki according to the protocol of the Internal Review Board of Kyoto University, which approved this study.

Patients

Patient 1 was an XL-EDA-ID patient with a duplication mutation of the *NEMO* gene spanning intron 3 to exon 6. This patient has been reported previously[17] and died from an *Aspergillus* infection at the age of 4. Patient 2, born at term, was the younger brother of patient 1. This patient was also diagnosed as XL-EDA-ID with the same duplication mutation as patient 1 by genetic study. He received trimethoprim-sulfamethoxazole prophylaxis and a monthly infusion of immunoglobulin from the age of 1 month. The patient maintained good health and had a body weight of 7899*g* at 6 months when he started to fail to thrive. Except for poor weight gain, patient 2 appeared active with a good appetite, negative C-reactive protein, normal white blood cell counts, and no apparent symptoms. At 19 months of age, *Mycobacterium szulgai* was detected by venous blood culture, and the patient was treated with multidrug regimens including ethambutol, rifabutin, and clarithromycin based on the treatment of systemic *Mycobacterium avium* complex infection. The patient responded well to the treatment and his weight increased from 7830*g* to 9165*g* within a month after the treatment was initiated. Patient 2 received an unrelated cord blood cell transplantation at 26 months of age, containing 8.5×10^7 nucleated cells/kg (4.4×10^5 $CD34^+$ cells/kg), which was matched at 5 of 8 loci: mismatches occurred at 1 HLA-B and 1 HLA-C allele (according to serology), and at 1 HLA-A, 1 HLA-B, and 1 HLA-C allele (according to DNA typing). The preconditioning regimen consisted of fludarabine (30 mg/m^2/d) on days −7 to −3, melphalan (70 mg/m^2/d) on days −6 to −5, and rabbit anti-thymocyte globulin (2.5 mg/kg/d) on days −6 to −2. At first, Tacrolimus (0.024 mg/kg/d) was used to prevent GVHD, but this was switched to cyclosporin A (3 mg/kg/d) on day 9 because of drug-induced encephalopathy. Neutrophil ($> 0.5 \times 10^9$/L) and platelet ($> 50 \times 10^9$/L) engraftment were examined on days 13 and 40, respectively. Although $CD19^+$ cells (2042/μL, 94% donor chimerism), $CD56^+$ cells (242/μL, 97% donor chimerism), and monocytes (557/μL, 69% donor chimerism) were successfully generated, $CD3^+$ cells were not detected in the peripheral blood by day 54. The patient suffered from septic shock and died on day 60. Patients 3 to 10 were XL-EDA-ID patients recruited nationwide in Japan. Clinical details of patients 3, 4, and 10 have been reported previously.[18-20] These patients had clinical phenotypes characteristic of XL-EDA-ID such as ectodermal dysplasia, innate and/or acquired immunity defects, and susceptibility to pyogenic bacteria and *Mycobacterium* infection. Every patient had a mutation in the *NEMO* gene that caused reduced NF-κB activation in a NEMO reconstitution assay, as described in "Proliferation of $NEMO^{normal}$ and $NEMO^{low}$ T cells." Patient profiles are listed in Table 1.

Flow cytometric analysis

NEMO intracellular staining was performed as previously described.[17] The cells were stained for the following lineage markers before staining for NEMO: CD4, CD8, CD14, CD15, CD19, CD56, CD45RA (BD Biosciences/BD Pharmingen), and CCR7 (R&D Systems Inc). Intracellular staining of human IFN-γ, TNF-α, and NEMO was performed as previously described.[18] The stained cells were collected using a FACSCalibur flow cytometer (BD Biosciences) and analyzed using the FlowJo software (TreeStar).

Reporter assay

Wild-type and mutant *NEMO* cDNAs were generated from a healthy volunteer and the recruited XL-EDA-ID patients by RT-PCR; the cDNAs were subcloned into the p3xFLAG-CMV14 vector (Sigma-Aldrich). NEMO null rat fibroblast cells (kindly provided by Dr S. Yamaoka, Department of Molecular Virology, Graduate School of Medicine, Tokyo Medical and Dental University, Tokyo, Japan) were plated at a density of

From bloodjournal.hematologylibrary.org at Hirosaki University on January 30, 2013. For personal use only.

3×10^4 cells/well in a 24-well culture dish and were transfected with 40 ng of NF-κB reporter plasmid (pNF-κB-Luc; BD Biosciences/BD Clontech), 2 ng of *NEMO* mutant expression construct, 10 ng of internal control for the normalization of transfection efficiency (pRL-TK; Toyo Ink), and 148 ng of mock vector using FuGENE HD Transfection Reagent (TOYO-B-Net) according to the manufacturer's protocol. Twelve hours after transfection, the cells were stimulated with 15 ng/mL lipopolysaccharide (LPS; Sigma-Aldrich) for 4 hours and the NF-κB activity was measured using the PicaGene Dual SeaPansy assay kit (TOYO-B-Net). Experiments were performed in triplicate and firefly luciferase activity was normalized to *Renilla* luciferase activity.

Subcloning analysis of cDNA

Cell sorting of the various cell lineages was performed by FACSVantage (BD Biosciences). The purity of each lineage was > 95%. The cDNA from sorted cells was purified and reverse transcribed by Super Script III (Invitrogen) with random hexamers and amplified by the proofreading PCR enzyme KOD, as previously described.[17,21] The PCR primers used were NEMO2 (5′-AGAGACGAAGGAGCACAAAGCTGCCTTGAG-3′) and NEMO3 (5′-ACTGCAGGGACAATGGTGGGTGCATCTGTC-3′). The PCR products were subcloned using a TA cloning kit (Invitrogen) and sequenced by ABI 3130xl Genetic analyzer (Applied Biosystems). To determine whether additional mutations occurred in revertant subclones that had wild-type sequence in the original mutation site, the entire coding region of the *NEMO* gene was sequenced and an additional mutation was considered present when the same mutation was detected in multiple subclones.

Allele-specific PCR

The mRNA purified from sorted T cells and monocytes was reverse-transcribed by SuperScript III (Invitrogen) with the gene-specific primer NEMO2 and amplified by the proofreading PCR enzyme KOD (Toyobo) using the primers NEMO3 and NEMO 4 (5′-TGTGGACACGCAGT-GAAACGTGGTCTGGAG-3′). The PCR products were used as templates for allele-specific PCRs with Ex Taq polymerase (Takara Bio). Mutant and wild-type *NEMO* DNA was generated from each NEMO expression plasmid, mixed at graded ratios, and used as controls. PCR conditions and primer sequences are listed in supplemental Table 1 (available on the *Blood* Web site; see the Supplemental Materials link at the top of the online article).

Proliferation of NEMO^{normal} and NEMO^{low} T cells

To obtain PHA-induced T-cell blasts, PBMCs were stimulated with PHA (1:100; Invitrogen) and cultured in RPMI 1640 supplemented with 5% FCS and recombinant human IL-2 (50 IU/mL; kindly provided by Takeda Pharmaceutical Company) at 37°C for 7 days. Subcloning analysis of the cDNA obtained from the T-cell blasts was performed as described in "Subcloning analysis of cDNA."

Results

Reversion mosaicism of NEMO occurred in siblings with similar immunologic phenotypes

We previously reported patient 1 with a duplication mutation of the *NEMO* gene spanning intron 3 to exon 6, who was diagnosed as XL-EDA-ID at 1 year of age after suffering from recurrent infections.[17] At first, genetic diagnosis of the patient was difficult because the expression of aberrant *NEMO* mRNA was masked by the expression of normal *NEMO* mRNA by the revertant cells. Flow cytometric analysis of intracellular NEMO expression revealed cells with normal (NEMO^{normal}) and reduced (NEMO^{low}) levels of NEMO expression, indicating the presence of reversion mosaicism of the *NEMO* gene, and further analysis revealed that the *NEMO* mutation was disease-causing. PCR across the mutated region and sequencing of the PCR products revealed a duplication extending from intron 3 to exon 6, which was confirmed by Southern blot analysis. Additional copy number analysis of the *NEMO* gene of patient 1 and his mother excluded the possibility of a complex chromosomal aberration such as multiple duplication of the *NEMO* gene (supplemental Figure 1). Furthermore, polymorphism analysis using variable number tandem repeats on NEMO^{normal} and NEMO^{low} cells from patient 1 revealed that these cells were derived from the same origin (supplemental Table 2), indicating that the *NEMO* gene mosaicism was less likely because of amalgamation. The genomic analysis of the NEMO^{normal} cells revealed a complete reversion of the *NEMO* gene with no additional mutations. The clinical phenotype of patient 1 was combined immunodeficiency with a reduced number of T cells and mitogen-induced proliferation (Tables 2-3). We previously determined that reduced NEMO expression in the mutant T cells caused impairment of T-cell development and mitogen-induced proliferation.

Patient 2, the younger brother of patient 1, was diagnosed as XL-EDA-ID with the same duplication mutation as his brother. Flow cytometric analysis of intracellular NEMO expression performed at diagnosis showed that most of his PBMCs had reduced NEMO expression (Figure 1A). At 2 months of age, when most of the T cells were NEMO^{low}, absolute counts of the patient's T cells and the mitogen-induced proliferation of the patient's PBMCs were comparable with those of the healthy controls (Figure 1A-B; Table 2). These findings indicated that the *NEMO* mutation had no effect on T-cell development and mitogen-induced proliferation during early infancy in patient 2.

NEMO^{normal} T cells gradually increased as patient 2 grew older, while the absolute count of NEMO^{low} T cells decreased (Figure 1A-B). Accordingly, normal full-length *NEMO* cDNA, which had been undetectable in cord blood, was detectable in the patient's peripheral blood at 12 months of age. However, while NEMO^{normal} T cells were increasing, mitogen-induced T-cell proliferation started to decrease (Table 3), and the patient started to show poor weight gain from 6 months of age. When patient 2 was 17 months old, a blood culture revealed an *M szulgai* bacteremia. At this time, the absolute count of NEMO^{normal} T cells peaked, and NEMO^{low} T cells were at a minimum. He began to gain weight after anti-*Mycobacterium* medication was initiated, although NEMO^{normal} T cells started to decrease and NEMO^{low} T cells began to increase (Figure 1B). When the patient was 23 months old, mitogen-induced T-cell proliferation was still low and a roughly equal number of NEMO^{low} and NEMO^{normal} T cells were detected (Table 3). Overall, as patient 2 grew older, NEMO^{normal} T cells increased as the total number of T cells and the mitogen-induced T-cell proliferation decreased, similar to what had occurred in patient 1 at a similar age.

Various analyses were performed to compare the immunologic phenotype of NEMO^{low} and NEMO^{normal} T cells in detail. Both NEMO^{normal} and NEMO^{low} CD4$^+$ T cells carried a diverse Vβ repertoire, but CD8$^+$ T cells had a skewed Vβ repertoire regardless of NEMO expression level (Figure 1C). Surface marker analysis revealed that most of the NEMO^{normal} T cells were CD45RA$^-$/CCR7$^-$ and most of the NEMO^{low} T cells were CD45RA$^+$/CCR7$^+$ (Figure 1D). The NEMO^{normal} T cells produced similar amounts of IFN-γ and TNF-α as healthy control cells, while the production of these cytokines were reduced in NEMO^{low} T cells (Figure 1E-F). Taken together, these data implied that the immunologic phenotype of T cells from patient 2 converged with that of patient 1 as patient 2 grew older.

From bloodjournal.hematologylibrary.org at Hirosaki University on January 30, 2013. For personal use only.

Table 2. Surface marker analysis of peripheral mononuclear cells of patients 1 and 2

	Patient 1	Patient 2		Healthy controls
Age at analysis	2 y	2 mo	19 mo	
CD3	1503	2366	1014	2997 ± 1751
CD4	292	1583	374	1683 ± 874
CD8	1160	783	547	1114 ± 976
TCRαβ	1386	2295	439	2620 ± 1612
TCRγδ	109	74	574	343 ± 177
CD4+CD45RA	58	1336	105	1471 ± 890
CD4+CD45RO	263	307	266	497 ± 189
CD8+CD45RA	1178	783	297	1083 ± 1078
CD8+CD45RO	361	21	250	385 ± 442
CD4+CD25	80	427	93	210 ± 99
CD19	1200	941	1543	1252 ± 1145
CD20	1189	931	1536	1125 ± 837
CD19+Sm-IgG	7	18	17	54 ± 21
CD19+Sm-IgA	15	4	14	18 ± 14
CD19+Sm-IgM	1171	910	1505	1057 ± 881
CD19+Sm-IgD	1171	906	1495	1052 ± 884
CD16	912	176	24	287 ± 200
CD56	908	176	24	306 ± 207

Surface markers expressed by XL-EDA-ID patients' PBMCs are shown as absolute counts per microliter of peripheral blood. Healthy control values are based on children aged 1 to 6 years and are shown as the mean ± SD.

Sm indicates the surface membrane.

High incidence of somatic mosaicism of the *NEMO* gene in XL-EDA-ID patients

It is worth noting that somatic reversion mosaicism of the *NEMO* gene occurred in both of the 2 XL-EDA-ID siblings carrying a duplication mutation. To determine whether a high frequency of reversion is a specific event for this type of *NEMO* duplication mutation[22-25] or if the reversion of the *NEMO* gene occurs commonly in XL-EDA-ID patients, we recruited an additional 8 XL-EDA-ID patients from throughout Japan (Table 1) and analyzed the presence of *NEMO* reversion. These patients had various combinations of clinical phenotypes characteristic of XL-EDA-ID such as ectodermal dysplasia, innate and acquired immunity defects, and susceptibility to pyogenic bacteria and *Mycobacterium* infections. Every patient had a mutation of the *NEMO* gene with reduced NF-κB activation potential, as evaluated in a NEMO reconstitution assay (Figure 2).

Among the 8 patients, only patient 3 had a large proportion of $NEMO^{low}$ cells by flow cytometric analysis. The majority of patient 3's PBMCs were $NEMO^{low}$, whereas 10% of the patient's $CD8^+$ cells were $NEMO^{normal}$ (Figure 3A). This patient was identified as carrying the D311E mutation. Because missense mutations of the *NEMO* gene often do not result in the reduced expression of NEMO protein, subcloning and sequencing analysis was performed on the *NEMO* cDNA isolated from the remaining patients, and 6 of the 7 patients had normal *NEMO* subclones (Table 3). Expansion of maternal cells after fetomaternal transfusion was ruled out in these patients by FISH analysis with X and Y probes (Table 1).

Additional genetic analysis of the entire coding region of the *NEMO* gene was performed on $NEMO^{normal}$ cells from patient 3 and on reverted subclones from the other patients, except for patient 10 who had already received stem cell transplantation. The *NEMO* gene in these samples had reverted to wild-type with no additional mutations (Figure 3B and data not shown). To specifically determine in which cell lineages the reversion occurred, subcloning and sequencing analysis of cDNA in various cell lineages was performed. This analysis revealed that all the revertant cells were of the T-cell lineage and that no reversion occurred in monocytes and very little occurred in B cells (Table 4). Allele-specific PCR confirmed that reversion occurred in T cells but not in monocytes (Figure 4).

Selective advantage of $NEMO^{normal}$ cells in XL-EDA-ID carriers

The high frequency of somatic mosaicism in T cells of XL-EDA-ID patients indicated a strong selective advantage of wild-type NEMO T cells over T cells carrying mutant NEMO. To confirm this hypothesis, *NEMO* cDNA analysis was performed on various cell lineages from the mothers of the patients who are heterozygous for *NEMO* mutation and thus have mosaicism

Table 3. Immunologic analysis of patients 1 and 2

	Patient 1	Patient 2 (treated with IVIG)	
Age at analysis, mo	9	9	20
Serum immunoglobulin levels, g/L (control)			
IgG	10.63 (4.51-10.46)	8.44 (4.51-10.46)	10.37 (7.15-9.07)
IgA	1.36 (0.14-0.64)	1.88 (0.14-0.64)	3.93 (0.22-1.44)
IgM	0.4 (0.33-1.00)	0.17 (0.33-1.00)	0.20 (0.34-1.28)
Age at analysis	2 y	2 mo	23 mo
T-cell proliferation, SI (control)	9.3 (206.9 ± 142.5)	55.3 (64.8 ± 8.1)	7.2 (89.4 ± 31.2)

Control values of serum immunoglobulin levels are based on children aged either 7 to 9 months or 1 to 2 years and are shown as the mean ± SD. The T-cell proliferation assay was performed as described previously[17] with at least three healthy adults as controls.

SI indicates stimulation index; and IVIG, 2.5 g of monthly IV immune globulin infusion.

From bloodjournal.hematologylibrary.org at Hirosaki University on January 30, 2013. For personal use only.

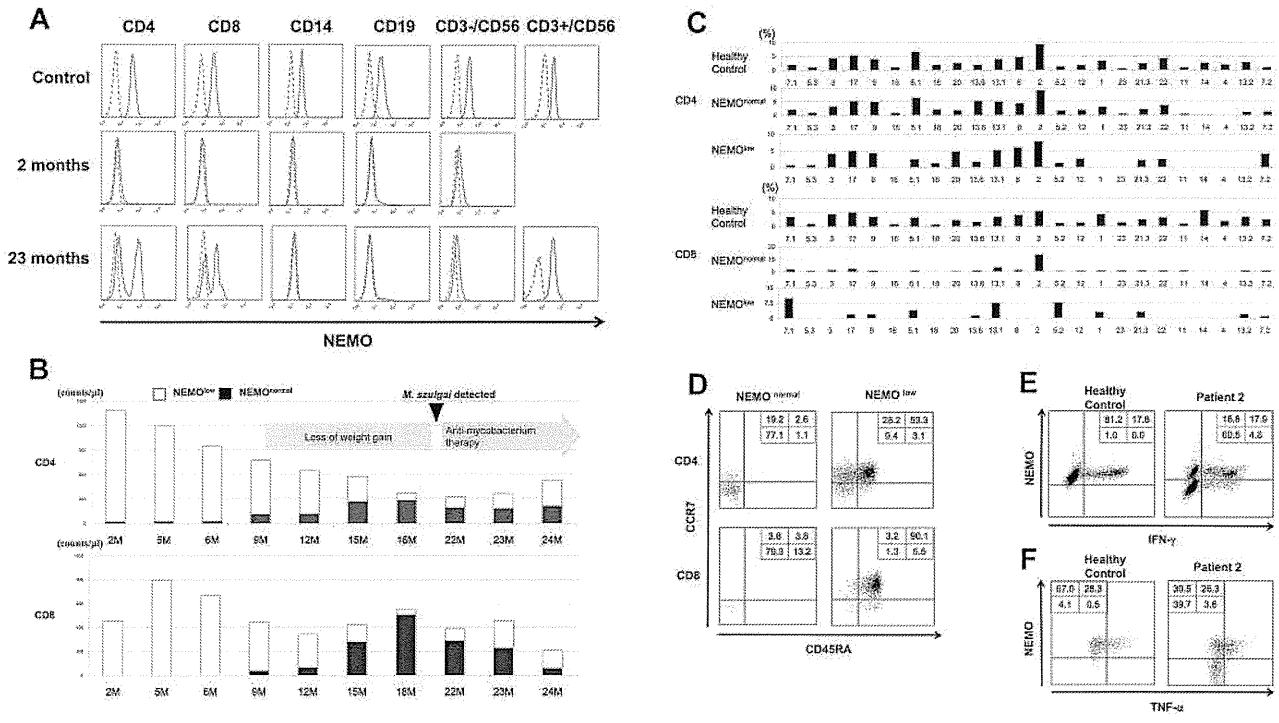

Figure 1. Identification and characterization of *NEMO* revertant T cells in patient 2. (A) Intracellular expression of NEMO in various PBMC lineages from a healthy adult control and patient 2 were evaluated by flow cytometry. For the patient, results of the analyses performed at 2 months and 23 months are shown. Solid lines indicate staining with the anti-NEMO mAb, and dotted lines indicate the isotype control. (B) Time-course variations in the absolute count of NEMO^{normal} and NEMO^{low} T cells in patient 2. M indicates age in months. (C) TCR-Vβ repertoire analysis of the patient's CD4$^+$ and CD8$^+$ T cells. PBMCs from the patient and a healthy adult control were stained for the TCR-Vβ panel, CD4, CD8, and NEMO, and analyzed by flow cytometry. (D) Phenotype analysis of T cells in patient 2. PBMCs from the patient and a control were stained for the expression of NEMO, CCR7, CD45RA, and CD4 or CD8. Data shown were gated on NEMO^{normal} or NEMO^{low} CD4$^+$ or CD8$^+$ cells. (E-F) Cytokine production from NEMO^{normal} and NEMO^{low} T cells. PBMCs from the patient and a control were stimulated with PMA and ionomycin for 6 hours and stained for intracellular (E) IFN-γ or (F) TNF-α along with NEMO. Cells shown are gated on the CD3$^+$ population.

because of X-chromosome inactivation. This analysis assumes that the percentage of cDNA for wild-type *NEMO* reflects the percentage of cells expressing wild-type NEMO. A high proportion of wild-type *NEMO* cDNA was observed in T cells from the mothers of patients 1/2, 3, 8, and 10, although wild-type *NEMO* cDNA was not predominant in T cells from the mother of patient 4 (Table 5).

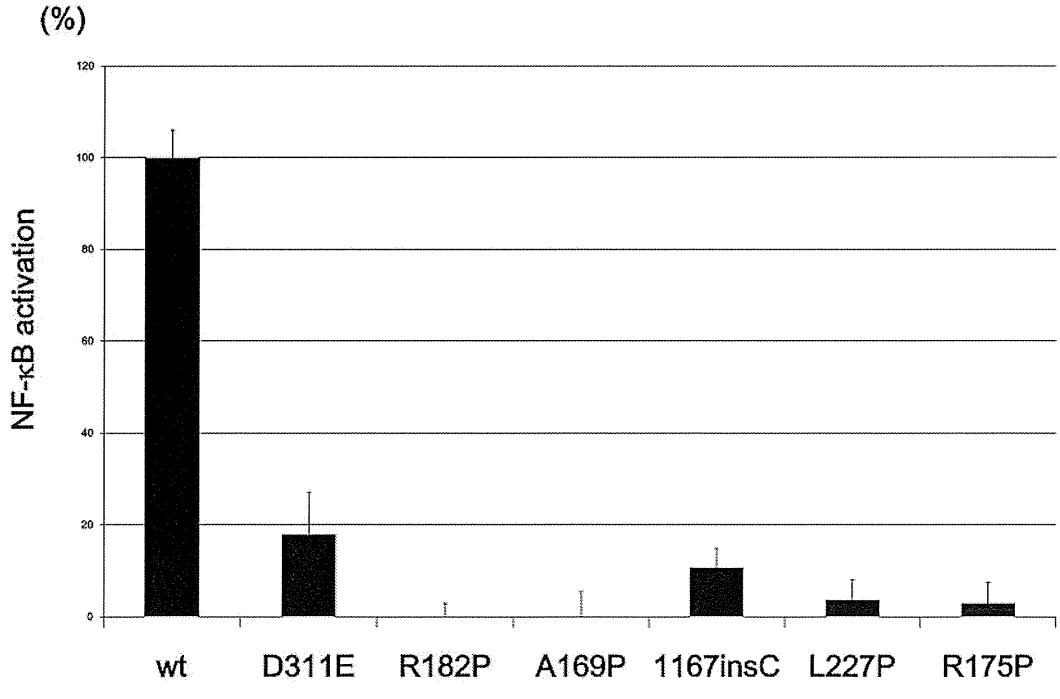

Figure 2. NF-κB transactivation by NEMO mutants from the XL-EDA-ID patients. NF-κB transactivation induced by NEMO mutants in the XL-EDA-ID patients. Mock vectors and wild-type (wt) NEMO were used as controls. The NF-κB activation index of NEMO variants were calculated as (NF-κB activation by each NEMO variant − NF-κB activation of the mock vector)/(NF-κB activation by wild-type NEMO − NF-κB activation of the mock vector). The data shown are the mean ± SD of triplicate wells and are representative of 3 independent experiments with similar results.

From bloodjournal.hematologylibrary.org at Hirosaki University on January 30, 2013. For personal use only.

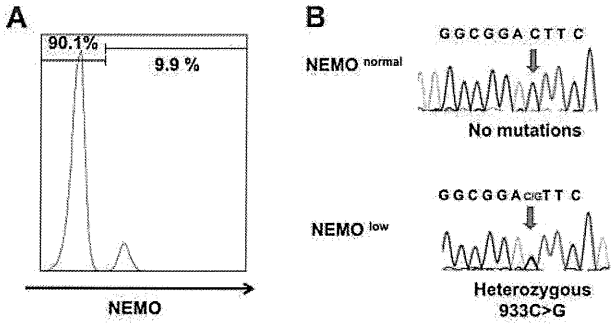

Figure 3. *NEMO* revertant T cells in patient 3. (A) Intracellular expression of NEMO in CD8+ cells from patient 3. (B) Sequencing chromatograms of DNA from NEMO^{normal} or NEMO^{low} CD8+ cells of patient 3. Arrows indicate the mutated base position at c. 931.

Similarly, there was an apparent high proportion of wild-type *NEMO* cDNA in monocytes and B cells from the mothers of patients 1/2, 8, and 10 (Table 5). These findings suggested a general selective advantage of NEMO^{normal} cells over NEMO^{low} cells in vivo, especially in T cells.

Proliferation capacity of NEMO^{normal} and NEMO^{low} T cells

T-cell proliferation stimulated by mitogens such as PHA is usually not reduced in XL-EDA-ID patients. However, the emergence of NEMO^{normal} cells coincided with a reduction in mitogen-induced proliferation in patient 2. To further determine the effect of NEMO^{normal} cells on mitogen-induced proliferation of peripheral T cells, the proportions of T cells carrying the wild-type and mutant were examined before and after PHA stimulation in XL-EDA-ID patients and their mothers (Table 6). In patients 2, 4, and 8, the percentage of the NEMO^{normal} cells decreased after PHA stimulation, while NEMO^{normal} cells prevailed in patient 9. In the mothers of patient 4 and 10, the percentage of NEMO^{normal} cells increased after PHA stimulation, while the percentage of the NEMO^{normal} cells decreased in the mother of patient 3. These results indicated that the NEMO mutation does not directly affect the mitogen-induced proliferation capacity of T cells and factors other than the *NEMO* genotype determine the proliferation capacity of NEMO^{normal} and NEMO^{low} T cells.

Discussion

Somatic reversion mosaicism has been described in several disorders affecting the hematopoietic system, the liver, and the skin.[23,26] Reports of somatic reversion cases have been particularly abundant in patients with immunodeficiency diseases, including Wiskott-Aldrich syndrome (WAS)[27] and SCID, which occur because of mutations in the interleukin receptor common γ chain,[28] CD3ζ,[29] *RAG-1*[30], and *ADA* genes.[31] Patients with somatic reversion mosaicism may present with significantly milder clinical phenotypes compared with nonrevertant patients with the same germline mutation, although this is not always the case.[26] One common feature in most cases where the somatic reversion mosaicism has been observed is a strong in vivo selective advantage of the revertant cells that express the wild-type gene product. One of the most intensively investigated diseases associated with somatic reversion mosaicism is WAS.[32-34] A report showed that up to 11% of WAS patients have presented with somatic reversion mosaicism.[33]

In our investigation, 9 of 10 XL-EDA-ID patients presented with somatic mosaicism. Two of the 9 were cases of reversion from a duplication mutation, while the others exhibited true back-reversion from a substitution or insertion mutation. This finding calls for caution when diagnosing XL-EDA-ID patients. Because the existence of a *NEMO* pseudogene makes it difficult to perform genetic analysis using genomic DNA, diagnosis of the disease is often confirmed by sequencing analysis of *NEMO* cDNA, and the presence of somatic mosaicism can cause misdiagnosis of XL-EDA-ID patients either when NEMO^{normal} cells make up the majority of the patients' PBMCs or when the cDNA of the mutated *NEMO* gene cannot be amplified by PCR.[17] In fact, mutated *NEMO* cDNA could not be amplified from the PBMCs of patient 2 even when NEMO^{normal} cells were absent (during early infancy), and only wild-type *NEMO* cDNA was amplified after the appearance of NEMO^{normal} cells (data not shown), probably because of the instability of the mutated *NEMO* mRNA. Flow cytometric analysis of intracellular NEMO protein is of help in identifying the NEMO^{low} cells in some patients, but the technique is not applicable when the *NEMO* mutation does not cause reduced expression of NEMO protein. Thus, some cases of XL-EDA-ID patients with reversion may be difficult to diagnose.

The high frequency of somatic mosaicism observed in XL-EDA-ID patients indicates a strong in vivo selective advantage for NEMO^{normal} cells, which express the wild-type gene product. Patient 2 presented with a high mutant T-cell count at birth that gradually decreased over time (Figure 1B). This finding indicates that wild-type NEMO expression is critical for the survival of certain cell lineages, including T cells, after birth. On the other hand, no NEMO^{normal} monocytes and very few NEMO^{normal} B cells were detected in the recruited XL-EDA-ID patients (Table 4). This specific feature is similar to other somatic reversion mosaicism seen in primary immunodeficiency patients[26] and indicates that the expression of NEMO is less critical for the survival of monocytes or B cells compared with that of T cells. There is also an apparent

Table 4. Analysis of *NEMO* gene mosaicism in various cell lineages for each patient

Patient	Mutation	Age at analysis	CD4, % (proportion)	CD8, % (proportion)	CD14, % (proportion)	CD19, % (proportion)
1	Duplication	2 y	90	100	0	4.0
2	Duplication	15 mo	45	66	0	4.0
3	D311E	3 y	2.4	9.9	0	1.2
4	A169P	12 y	0 (0/19)	24 (9/37)	0 (0/19)	0 (0/47)
5	L227P	3 y	0 (0/25)	0 (0/35)	0 (0/30)	0 (0/25)
6	R182P	4 y	18 (5/28)	17 (9/52)	0 (0/27)	0 (0/33)
7	R175P	6 y	0.4 (1/25)	39 (11/28)	0 (0/28)	0 (0/25)
8	Q348X	8 y	38 (6/16)	47 (9/19)	0 (0/33)	0 (0/25)
9	R175P	15 y	30 (9/30)	36 (12/33)	0 (0/23)	0 (0/14)
10	1167 ins C	9 mo		PBMC 9.3 (4/43)		

For patients 1 to 3, data represent the percentages of NEMO^{normal} cells in each lineage, as assessed by flow cytometry. For patients 4 to 10, the ratio indicates the number of wild-type NEMO clones in various cell lineages as compared with the total number of clones analyzed, based on subcloning and sequencing analysis.

From bloodjournal.hematologylibrary.org at Hirosaki University on January 30, 2013. For personal use only.

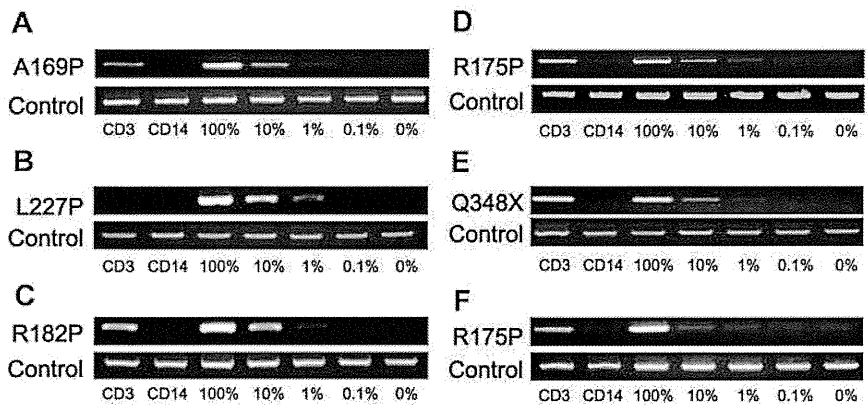

Figure 4. NEMO reversion selectively occurs in T cells of XL-EDA-ID patients. Allele-specific PCR for *NEMO* on CD3+ or CD14+ cells from (A) patient 4, (B) patient 5, (C) patient 6, (D) patient 7, (E) patient 8, and (F) patient 9. Numbers below each figure indicate the percentages of wild-type NEMO cDNA mixed with each mutant. Primers used in each PCR are shown on the left.

concordance between the degree of the disruption of *NEMO* gene and the proportion of reverted NEMO^{normal} cells compared with NEMO^{low} cells. The high proportion of reverted T cells seen in patients 1 and 2 as well as in patient 8 was associated with a highly disruptive mutation of the *NEMO* gene (ie, a duplication mutation in patients 1 and 2, and a truncation mutation in patient 8). In addition, the highly selective X-chromosome inactivation observed in the mothers of XL-EDA-ID patients indicated a strong selective advantage for NEMO^{normal} cells over NEMO^{low} cells. It is also noteworthy that reverted T cells were not detected in patient 5, who carried an L227P mutation that was not localized to either of the functional domains in the NEMO protein. Other reported cases with the same mutation presented with polysaccharide-specific humoral immunodeficiency and autoinflammatory diseases, but were spared complications such as cellular immunodeficiency and susceptibility to *Mycobacterium* (similar to patient 5).[4,8] This may reflect the fact that the L227P mutation in NEMO has less influence on T-cell growth than NEMO mutations that occur in functional domains, and suggests that reversion of the mutation has little impact on T-cell survival. Although the number of cases in our study is limited, it appears that the more disruptive NEMO mutations favor the survival of NEMO^{normal} cells after reversion and X-chromosome inactivation.

Regarding the gradual decline in the number of NEMO-deficient T cells, one candidate trigger could be infection. Because the dominance of the memory phenotype and the skewed TCR repertoire among CD8+ T cells in NEMO^{normal} cells were observed in both patients 1 and 2 (Figure 1C and Mizukami et al[18]), continuous infection of pyogenic bacteria in patient 1 and *M szulgai* in patient 2 could be a reason for the emergence of NEMO^{normal} cells and the elimination of NEMO^{low} cells. The decrease in NEMO^{normal} cells and restoration of NEMO^{low} cells after anti-mycobacterial therapy in patient 2 support this hypothesis. In the case of patient 1, the predominance of NEMO^{normal} T cells with an effector/memory phenotype at diagnosis (Table 4 and Mizukami et al[18]) is likely to be the result of chronic infection, and it is possible that NEMO^{low} cells were predominant during his early infancy. Because some reports have indicated that TNF-α–induced programmed cell death of several cell types, including a human T-cell line, was enhanced by hypomorphic *NEMO* mutations,[12,35] and considering our finding that the levels of TNF-α expressed in revertant T cells were similar to levels in healthy control T cells in vitro (Figure 1F), TNF-α produced from these cells in response to infection could be involved in mutant T-cell elimination.

Unexpectedly, T-cell proliferation in patient 2 was equivalent to that of normal controls at the age of 2 months and was reduced after NEMO^{normal} T cells increased (Figure 1B; Table 3). This finding indicates that the NEMO^{low} T cells did not have intrinsically impaired mitogen-induced proliferation. One reasonable explanation for the reduced proliferation observed after the increase in NEMO^{normal} T cells is a reduction in the absolute number of T cells (naive T cells in particular), probably because of the infection.

Table 5. Expression of mutant NEMO in various cell lineages for the mother of each XL-EDA-ID patient

Sample	Mutation	Analysis	Subtype	Mutant type, % (proportion)
Mother of patients 1 and 2	Duplication	FACS	CD3	0
			CD14	0
			CD19	0
Mother of patient 3	D311E	FACS	CD3	13
			CD3−	54
		Subcloning	CD3	22 (6/27)
			CD3−	55 (12/22)
Mother of patient 4	A169P	Subcloning	CD3	52 (11/21)
			CD14	58 (11/19)
			CD19	42 (5/12)
Mother of patient 8	Q348X	Subcloning	CD3	0 (0/26)
			CD14	17 (3/18)
			CD19	0 (0/18)
Mother of patient 10	1167insC	Subcloning	CD3	18 (7/39)
			CD14	12 (5/43)
			CD19	27 (12/44)

Data are shown as either the percentages of NEMO^{normal} cells, as assessed by flow cytometry, or as the ratio of clones containing wild-type NEMO to the total number of clones, as analyzed by subcloning and sequencing analysis.

From bloodjournal.hematologylibrary.org at Hirosaki University on January 30, 2013. For personal use only.

Table 6. Expression of mutant NEMO in CD3-positive cells and PHA blasts

Sample	Mutations	Analysis	Subtype	Mutant type, % (proportion)
Mother of patient 3	D311E	FACS	CD3	13
			PHA blast	47
		Subcloning	CD3	22 (6/27)
			PHA blast	48 (11/23)
Mother of patient 4	A169P	Subcloning	CD3	52 (11/21)
			PHA blast	18 (9/49)
Mother of patient 8	Q348X	Subcloning	CD3	0 (0/26)
			PHA blast	0 (0/21)
Mother of patient 10	1167insC	Subcloning	CD3	18 (7/39)
			PHA blast	9 (4/43)
Patient 2	Duplication	FACS	CD3	73
			PHA blast	93
Patient 4	A169P	Subcloning	CD3	79 (19/24)
			PHA blast	100 (37/37)
Patient 8	Q348X	Subcloning	CD3	56 (18/32)
			PHA blast	100 (16/16)
Patient 9	R175P	Subcloning	CD3	87 (34/39)
			PHA blast	0 (0/28)

PHA blasts were obtained by incubating PBMCs with PHA and soluble IL-2 for 7 days. Data are shown as either the percentages of $NEMO^{normal}$ cells, as assessed by flow cytometry, or as the ratio of clones containing wild-type NEMO to the total number of clones, as analyzed by subcloning and sequencing analysis.

Therefore, to identify other mechanisms underlying reduced T-cell proliferation, the impact of *NEMO* mutation on PHA-induced T-cell proliferation was indirectly examined in vitro by comparing the response of $NEMO^{normal}$ and $NEMO^{low}$ cells derived from XL-EDA-ID patients and their mothers. After PHA stimulation and proliferation, the proportion of $NEMO^{low}$ T cells increased in patients 2, 4, and 8, while the opposite result was observed in patient 9 and in the mother of patient 4 (Table 6). Although the precise mechanism is unclear, a reduction in the proportion of $NEMO^{normal}$ cells after PHA stimulation would reflect the lower proliferative capacity of $NEMO^{normal}$ cells compared with that of $NEMO^{low}$ cells, which may be another explanation for the reduced T-cell proliferation observed in patient 2 at 23 months of age when $NEMO^{normal}$ T cells were dominant. In the reports on reversion mosaicism of *IL2RG* gene mutations,[28,36] the restoration of T-cell function and clinical symptoms varied among patients. Therefore, other factors besides the genotype of the mutations, such as the developmental stage where reversion occurred and the frequency of reversion, affect the clinical impact of somatic mosaicism of *NEMO* gene mutations.

In this study, the effect of somatic mosaicism of the *NEMO* gene on clinical phenotype could not be fully evaluated. However, cytokines produced by revertant T cells could influence the development of clinical symptoms of XL-EDA-ID, such as inflammatory bowel disease. In a mouse model, intestinal epithelial cell-specific inhibition of NF-κB through the conditional ablation of NEMO resulted in the development of chronic bowel inflammation sensitized intestinal epithelial cells to TNF-α–induced apoptosis.[37] In this model, the first phase of intestinal inflammation was initiated by epithelial cell death and was followed by a second phase of TNF-α–induced intestinal inflammation, the latter being dependent on T cells. Another report showed that HSCT in XL-EDA-ID patients exacerbated the patients' inflammatory bowel disease.[38] Indeed, in patient 4, the percentage of reverted T cells was reduced after repeated administrations of anti-TNFα blocking Ab, and the symptoms of inflammatory bowel disease improved.[18] Considering this evidence, somatic mosaicism in T cells might be an important factor leading to inflammatory disease in XL-EDA-ID patients with defective NF-κB activation. However, our study did not show a tight association between inflammatory bowel disease and somatic mosaicism, and further investigation is needed to determine whether the $NEMO^{normal}$ T cells play a role in inflammatory processes in XL-EDA-ID.

In conclusion, this study has identified a high frequency of somatic mosaicism in XL-EDA-ID patients, particularly in T cells, and has revealed important insights into human T-cell immunobiology in XL-EDA-ID. Although we could not demonstrate the clinical impact of somatic mosaicism in XL-EDA-ID patients, our findings suggest that care is required when making molecular diagnoses of XL-EDA-ID, and might shed light on the mechanisms underlying the variability in the clinical manifestation of XL-ED-ID and facilitate the search for appropriate treatments.

Acknowledgments

The authors are grateful to all the XL-EDA-ID patients and their families for their participation. They also thank Shoji Yamaoka (Department of Molecular Virology, Graduate School of Medicine, Tokyo Medical and Dental University, Tokyo, Japan) for kindly providing NEMO-null rat fibroblast cells, and Takeda Pharmaceutical Company Limited for kindly providing the recombinant human IL-2.

This work was supported by grants from the Japanese Ministry of Education, Culture, Sports, Science, and Technology, and by grants from the Japanese Ministry of Health, Labor and Welfare.

Authorship

Contribution: Tomoki Kawai wrote the manuscript and performed research; R.N., T.Y., T.N., and T.H. edited the manuscript and supervised this work; K.I., Y.M., N.T., H.S., M.S., and Y.T. cultured cells; and T. Mizukami, H.N., Y.K., A.Y., T. Murata, S.S., E.I., H.A., Toshinao Kawai, C.I., S.O., and M.K. treated patients and analyzed data.

Conflict-of-interest disclosure: The authors declare no competing financial interests.

Correspondence: Ryuta Nishikomori, MD, PhD, Department of Pediatrics, Kyoto University Graduate School of Medicine, 54 Kawahara-cho, Shogoin, Sakyo-ku, Kyoto 606-8507, Japan; e-mail: rnishiko@kuhp.kyoto-u.ac.jp.

From bloodjournal.hematologylibrary.org at Hirosaki University on January 30, 2013. For personal use only.

References

1. Pinheiro M, Freire-Maia N. Ectodermal dysplasias: a clinical classification and a causal review. *Am J Med Genet.* 1994;53(2):153-162.
2. Abinun M, Spickett G, Appleton AL, Flood T, Cant AJ. Anhidrotic ectodermal dysplasia associated with specific antibody deficiency. *Eur J Pediatr.* 1996;155(2):146-147.
3. Sitton JE, Reimund EL. Extramedullary hematopoiesis of the cranial dura and anhidrotic ectodermal dysplasia. *Neuropediatrics.* 1992;23(2):108-110.
4. Schweizer P, Kalhoff H, Horneff G, Wahn V, Diekmann L. [Polysaccharide specific humoral immunodeficiency in ectodermal dysplasia. Case report of a boy with two affected brothers]. *Klin Padiatr.* 1999;211(6):459-461.
5. Abinun M. Ectodermal dysplasia and immunodeficiency. *Arch Dis Child.* 1995;73(2):185.
6. Zonana J, Elder ME, Schneider LC, et al. A novel X-linked disorder of immune deficiency and hypohidrotic ectodermal dysplasia is allelic to incontinentia pigmenti and due to mutations in IKK-gamma (NEMO). *Am J Hum Genet.* 2000;67(6):1555-1562.
7. Courtois G, Smahi A, Israel A. NEMO/IKK gamma: linking NF-kappa B to human disease. *Trends Mol Med.* 2001;7(10):427-430.
8. Doffinger R, Smahi A, Bessia C, et al. X-linked anhidrotic ectodermal dysplasia with immunodeficiency is caused by impaired NF-kappaB signaling. *Nat Genet.* 2001;27(3):277-285.
9. Rothwarf DM, Zandi E, Natoli G, Karin M. IKK-gamma is an essential regulatory subunit of the IkappaB kinase complex. *Nature.* 1998;395(6699):297-300.
10. Yamaoka S, Courtois G, Bessia C, et al. Complementation cloning of NEMO, a component of the IkappaB kinase complex essential for NF-kappaB activation. *Cell.* 1998;93(7):1231-1240.
11. Smahi A, Courtois G, Vabres P, et al. Genomic rearrangement in NEMO impairs NF-kappaB activation and is a cause of incontinentia pigmenti. The International Incontinentia Pigmenti (IP) Consortium. *Nature.* 2000;405(6785):466-472.
12. Hanson EP, Monaco-Shawver L, Solt LA, et al. Hypomorphic nuclear factor-kappaB essential modulator mutation database and reconstitution system identifies phenotypic and immunologic diversity. *J Allergy Clin Immunol.* 2008;122(6):1169-1177.
13. Orange JS, Jain A, Ballas ZK, Schneider LC, Geha RS, Bonilla FA. The presentation and natural history of immunodeficiency caused by nuclear factor kappaB essential modulator mutation. *J Allergy Clin Immunol.* 2004;113(4):725-733.
14. Jain A, Ma CA, Liu S, Brown M, Cohen J, Strober W. Specific missense mutations in NEMO result in hyper-IgM syndrome with hypohydrotic ectodermal dysplasia. *Nat Immunol.* 2001;2(3):223-228.
15. Orange JS, Brodeur SR, Jain A, et al. Deficient natural killer cell cytotoxicity in patients with IKK-gamma/NEMO mutations. *J Clin Invest.* 2002;109(11):1501-1509.
16. Sebban H, Courtois G. NF-kappaB and inflammation in genetic disease. *Biochem Pharmacol.* 2006;72(9):1153-1160.
17. Nishikomori R, Akutagawa H, Maruyama K, et al. X-linked ectodermal dysplasia and immunodeficiency caused by reversion mosaicism of NEMO reveals a critical role for NEMO in human T-cell development and/or survival. *Blood.* 2004;103(12):4565-4572.
18. Mizukami T, Obara M, Nishikomori R, et al. Successful treatment with infliximab for inflammatory colitis in a patient with X-linked anhidrotic ectodermal dysplasia with immunodeficiency. *J Clin Immunol.* 2012;32(1):39-49.
19. Imamura M, Kawai T, Okada S, et al. Disseminated BCG infection mimicking metastatic nasopharyngeal carcinoma in an immunodeficient child with a novel hypomorphic NEMO mutation. *J Clin Immunol.* 2011;31(5):802-810.
20. Tono C, Takahashi Y, Terui K, et al. Correction of immunodeficiency associated with NEMO mutation by umbilical cord blood transplantation using a reduced-intensity conditioning regimen. *Bone Marrow Transplant.* 2007;39(12):801-804.
21. Saito M, Nishikomori R, Kambe N, et al. Disease-associated CIAS1 mutations induce monocyte death, revealing low-level mosaicism in mutation-negative cryopyrin-associated periodic syndrome patients. *Blood.* 2008;111(4):2132-2141.
22. Yang TP, Stout JT, Konecki DS, Patel PI, Alford RL, Caskey CT. Spontaneous reversion of novel Lesch-Nyhan mutation by HPRT gene rearrangement. *Somat Cell Mol Genet.* 1988;14(3):293-303.
23. Zhang LH, Jenssen D. Reversion of the hprt mutant clone SP5 by intrachromosomal recombination. *Carcinogenesis.* 1992;13(4):609-615.
24. Monnat RJ Jr, Chiaverotti TA, Hackmann AF, Maresh GA. Molecular structure and genetic stability of human hypoxanthine phosphoribosyltransferase (HPRT) gene duplications. *Genomics.* 1992;13(3):788-796.
25. Rautenstrauss B, Liehr T, Fuchs C, et al. Mosaicism for Charcot-Marie-Tooth disease type 1A: onset in childhood suggests somatic reversion in early developmental stages. *Int J Mol Med.* 1998;1(2):333-337.
26. Wada T, Candotti F. Somatic mosaicism in primary immune deficiencies. *Curr Opin Allergy Clin Immunol.* 2008;8(6):510-514.
27. Ariga T, Kondoh T, Yamaguchi K, et al. Spontaneous in vivo reversion of an inherited mutation in the Wiskott-Aldrich syndrome. *J Immunol.* 2001;166(8):5245-5249.
28. Stephan V, Wahn V, Le Deist F, et al. Atypical X-linked severe combined immunodeficiency due to possible spontaneous reversion of the genetic defect in T cells. *N Engl J Med.* 1996;335(21):1563-1567.
29. Rieux-Laucat F, Hivroz C, Lim A, et al. Inherited and somatic CD3zeta mutations in a patient with T-cell deficiency. *N Engl J Med.* 2006;354(18):1913-1921.
30. Wada T, Toma T, Okamoto H, et al. Oligoclonal expansion of T lymphocytes with multiple second-site mutations leads to Omenn syndrome in a patient with RAG1-deficient severe combined immunodeficiency. *Blood.* 2005;106(6):2099-2101.
31. Hirschhorn R. In vivo reversion to normal of inherited mutations in humans. *J Med Genet.* 2003;40(10):721-728.
32. Wada T, Schurman SH, Jagadeesh GJ, Garabedian EK, Nelson DL, Candotti F. Multiple patients with revertant mosaicism in a single Wiskott-Aldrich syndrome family. *Blood.* 2004;104(5):1270-1272.
33. Stewart DM, Candotti F, Nelson DL. The phenomenon of spontaneous genetic reversions in the Wiskott-Aldrich syndrome: a report of the workshop of the ESID Genetics Working Party at the XIIth Meeting of the European Society for Immunodeficiencies (ESID). Budapest, Hungary October 4-7, 2006. *J Clin Immunol.* 2007;27(6):634-639.
34. Davis BR, Yan Q, Bui JH, et al. Somatic mosaicism in the Wiskott-Aldrich syndrome: molecular and functional characterization of genotypic revertants. *Clin Immunol.* 2010;135(1):72-83.
35. Yamaoka S, Inoue H, Sakurai M, et al. Constitutive activation of NF-kappa B is essential for transformation of rat fibroblasts by the human T-cell leukemia virus type I Tax protein. *EMBO J.* 1996;15(4):873-887.
36. Speckmann C, Pannicke U, Wiech E, et al. Clinical and immunologic consequences of a somatic reversion in a patient with X-linked severe combined immunodeficiency. *Blood.* 2008;112(10):4090-4097.
37. Nenci A, Becker C, Wullaert A, et al. Epithelial NEMO links innate immunity to chronic intestinal inflammation. *Nature.* 2007;446(7135):557-561.
38. Fish JD, Duerst RE, Gelfand EW, Orange JS, Bunin N. Challenges in the use of allogeneic hematopoietic SCT for ectodermal dysplasia with immune deficiency. *Bone Marrow Transplant.* 2009;43(3):217-221.

From bloodjournal.hematologylibrary.org at Hirosaki University on March 15, 2012. For personal use only.

Brief report

Identification of *TRIB1* R107L gain-of-function mutation in human acute megakaryocytic leukemia

Takashi Yokoyama,[1] Tsutomu Toki,[2] Yoshihiro Aoki,[2] Rika Kanezaki,[2] Myoung-ja Park,[3] Yohei Kanno,[1] Tomoko Takahara,[1] Yukari Yamazaki,[1] Etsuro Ito,[2] Yasuhide Hayashi,[3] and Takuro Nakamura[1]

[1]Division of Carcinogenesis, Cancer Institute, Japanese Foundation for Cancer Research, Tokyo, Japan; [2]Department of Pediatrics, Hirosaki University Graduate School of Medicine, Hirosaki, Japan; and [3]Department of Hematology/Oncology, Gunma Children's Medical Center, Gunma, Japan

***Trib1* has been identified as a myeloid oncogene in a murine leukemia model. Here we identified a *TRIB1* somatic mutation in a human case of Down syndrome–related acute megakaryocytic leukemia. The mutation was observed at well-conserved arginine 107 residue in the pseudokinase domain. This R107L mutation remained in leukocytes of the remission stage in which *GATA1* mutation disappeared, suggesting the *TRIB1* mutation is an earlier genetic event in leukemogenesis. The bone marrow transfer experiment showed that acute myeloid leukemia development was accelerated by transducing murine bone marrow cells with the R107L mutant in which enhancement of ERK phosphorylation and C/EBPα degradation by Trib1 expression was even greater than in those expressing wild-type. These results suggest that TRIB1 may be a novel important oncogene for Down syndrome–related acute megakaryocytic leukemia. (*Blood.* 2012; 119(11):2608-2611)**

Introduction

The Down syndrome (DS) patients are predisposed to developing myeloid leukemia, and those patients frequently exhibit *GATA1* mutations.[1] However, it is proposed that the *GATA1* mutation is important for transient leukemia in DS but not sufficient for full-blown leukemia, suggesting that additional genetic alterations are needed.[1] Therefore, it is important to search the subsequent genetic changes for DS-related leukemia (ML-DS) to predict malignant transformation and prognosis of the patients.

Trib1 has been identified as a myeloid oncogene that cooperates with *Hoxa9* and *Meis1* in murine acute myeloid leukemia (AML).[2] As a member of the tribbles family of proteins, TRIB1 interacts with MEK1 and enhances ERK phosphorylation.[2,3] Moreover, TRIB1 promotes degradation of C/EBP family transcription factors, including C/EBPα, an important tumor suppressor for AML, and we observed that degradation of C/EBPα by Trib1 is mediated by its interaction with MEK1.[4] Thus, TRIB1 plays an important role in the development of AML by modulating both the RAS/MAPK pathway and C/EBPα function together with Trib2 that has also been identified as a myeloid-transforming gene.[5] Potential involvement of *TRIB1* in human leukemia has been reported in cases of AML with 8q34 amplification in which both *c-MYC* and *TRIB1* are included in the amplicon.[6] The enhancing effect of TRIB1 on the MAPK signaling suggests that TRIB1 alterations may be related to AML cases, which do not show any mutations in the pathway members, such as FLT3, c-Kit, or Ras. In this report, we identified a novel somatic mutation of *TRIB1* in a case of human acute megakaryocytic leukemia developed in DS (DS-AMKL). Retrovirus-mediated gene transfer followed by bone marrow transfer indicated that the mutation enhanced leukemogenic activity and MAPK phosphorylation by TRIB1.

Methods

Patients

TRIB1 mutations have been investigated in 12 cases of transient leukemia (TL), 5 of DS-AMKL, and 4 cell lines of DS-AML. Peripheral blood leukocytes of TL and bone marrow cells of DS-AMKL were used as sources for the molecular analysis. This study was approved by the Ethics Committee of Hirosaki University Graduate School of Medicine, and all clinical samples were obtained with informed consent from the parents of all patients, in accordance with the Declaration of Helsinki.

Patient 84 showed trisomy 21 and extensive leukocytosis at birth. Hematologic findings revealed the white blood cell count to be 148×10^9/L, including 87% myeloblasts, a hemoglobin level of 19.4 g/dL, and a platelet count of 259×10^9/L. Patent ductus arteriosus and atrial septal defect have been pointed out. Based on the hematologic data and the chromosomal abnormality, the patient was diagnosed as DS-related TL. The hematologic abnormality was then improved, but 8 months later 3% of 6.9×10^9/L white blood cells became myeloblasts (Figure 1A). A karyotype analysis of bone marrow cells revealed 48, XY,+8,+21 in 3 of 20 cells. In addition, *GATA1* mutation was detected at nt 113 from A to G, resulting in loss of the first methionine.[7] He was diagnosed as AMKL at this time, and his disease was in remission by subsequent chemotherapy.

PCR and sequencing

The entire coding region of human *TRIB1* cDNA of patients' samples was amplified using Taq polymerase (Promega) and specific primer pairs (the sequences of the primers are available on request). The genomic DNA samples of patient 84 were also analyzed. The sequence analysis of *GATA1* was performed as described previously.[7] After checking the PCR products by agarose gel electrophoresis, the products were purified and directly sequenced.

Submitted December 12, 2010; accepted January 6, 2012. Prepublished online as *Blood* First Edition paper, January 31, 2012; DOI 10.1182/blood-2010-12-324806.

The online version of this article contains a data supplement.

The publication costs of this article were defrayed in part by page charge payment. Therefore, and solely to indicate this fact, this article is hereby marked "advertisement" in accordance with 18 USC section 1734.

© 2012 by The American Society of Hematology

From bloodjournal.hematologylibrary.org at Hirosaki University on March 15, 2012. For personal use only.

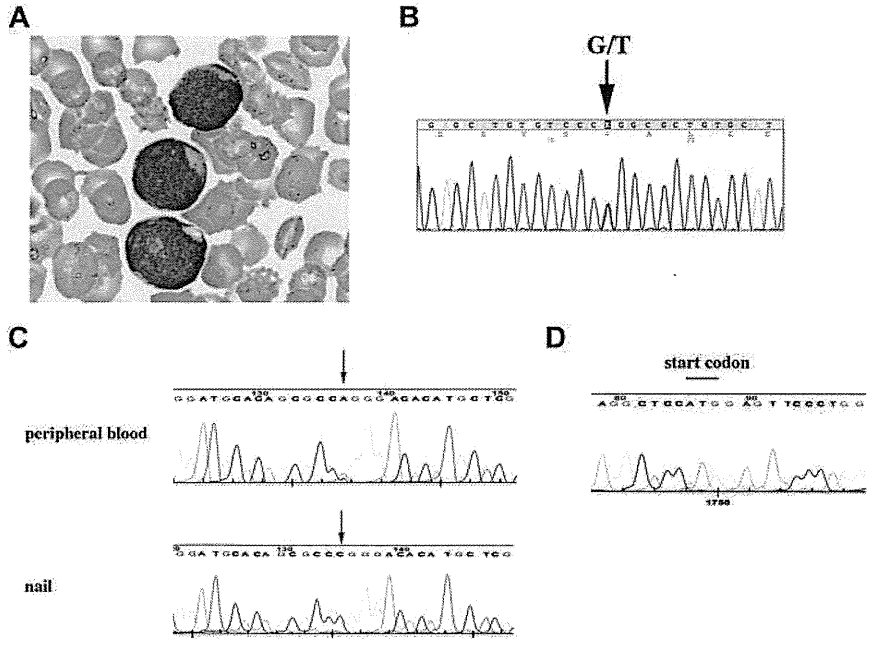

Figure 1. *TRIB1* R107L mutation identified in DS-related leukemias. (A) Giemsa staining of the case 84 peripheral blood smear diagnosed as AMKL. The image was acquired using a BX40 microscope equipped with a 100×/1.30 NA oil objective (Olympus) and a C-4040 digital camera (Olympus). (B) Fluorescent dye sequencing chromatographs of *TRIB1* genotyping by direct sequencing of the case 84 using a cDNA sample as a template. The vertical arrow indicates mixed G and T signals at codon 107. (C) Fluorescent dye sequencing chromatographs of *TRIB1* of peripheral blood leukocytes (top) or nail (bottom) in the same case at the complete remission stage. The red arrows indicate that the mutation remains in leukocytes but not in nail. The reverse strand sequences are shown. (D) *GATA1* sequence. The start codon that was mutated in AMKL[7] is normal in the peripheral blood leukocytes at the remission stage.

Retroviral infection of murine bone marrow cells and bone marrow transfer

Bone marrow cells were prepared from 8-week-old female C57Bl/6J mice 5 days after injection of 150 mg/kg body weight of 5-fluorouracil (Kyowa Hakko Kogyo). Retroviral infection of bone marrow cells and bone marrow transfer experiments were performed as described.[2] Transduction efficiencies evaluated by flow cytometric techniques were comparable between wild-type (WT; 5.3%) and R107L (3.4%). Animals were housed, observed daily, and handled in accordance with the guidelines of the animal care committee at Japanese Foundation for Cancer Research. All the diseased mice were subjected to autopsy and analyzed morphologically, and the blood was examined by flow cytometric techniques. The mice were diagnosed as positive for AML according to the classification of the Bethesda proposal.[8] The survival rate of each group was evaluated using the Kaplan-Meier method, and differences between survival curves were compared using the log-rank test.

Immunoblotting

Immunoblotting was performed using cell lysates in RIPA buffer as described.[4] Anti-p44/42 ERK (Cell Signaling Technologies), anti–phospho-p44/42 ERK (Cell Signaling Technologies), anti-C/EBPα (Santa Cruz Biotechnology), anti-FLAG (Sigma-Aldrich), and anti-GAPDH (Hy Test Ltd) antibodies were used.

Results and discussion

The important role of TRIB1 on the MAPK signaling suggests that *TRIB1* alterations may occur in some AML cases, which do not show overlapping mutations in the pathway members, such as FLT3, KIT, or RAS. Therefore, we tried to search mutations of *TRIB1* in cases of ML-DS and TL in which such mutations are infrequent.[9] In a case of DS-AMKL (case 84), a nucleotide change from guanine to thymine has been identified at 902 that results in amino acid alteration from arginine 107 (R107) to leucine (Figure 1B). The sequence changes were confirmed by subcloning the PCR product into the TA-type plasmid vector (data not shown). The nucleotide change was not observed in the DNA sample derived from the nail of the same patient at all (Figure 1C), indicating that this change is a somatic mutation. Interestingly, the mutation was retained in the peripheral blood sample in the complete remission stage in which the GATA1 mutation completely disappeared (Figure 1C-D). These results indicate that the *TRIB1* mutation precedes the onset of TL and the *GATA1* mutation, and suggest that *TRIB1* mutation occurred at the hematopoietic stem cell level and that the clone retaining the *TRIB1* mutation survived after chemotherapy. In case 84, there was no mutation for *FLT3* exons 14, 15, and 20, *PTPN11* exons 3 and 13, *KRAS* exons 2, 3, and 5, and *KIT* exons 8, 11, and 17 by the high-resolution melt analysis (data not shown).

An additional mutation was found in a case of TL (case 109) at the nucleotides 805 and 806 from GC to AT, which results in amino acid conversion from alanine (A75) to isoleucine (supplemental Figure 1, available on the *Blood* Web site; see the Supplemental Materials link at the top of the online article). *TRIB1* expression in DS-related and DS-unrelated leukemias was examined by real-time quantitative RT-PCR (supplemental Figure 2).

R107 is located within a psuedokinase domain of TRIB1 that is considered as a functionally core domain of TRIB family proteins.[10] Sequence comparison among 3 TRIB family proteins as well as tribbles homologs in other organisms revealed that the R107 is well conserved in mammalian TRIB1 and TRIB2,[10] suggesting that this arginine residue is evolutionary conserved and may be related to an important function. On the other hand, A75 is located outside of the pseudokinase domain, not conserved between human and mouse, or other tribbles homologs. Moreover, the N-terminal domain containing A75 is dispensable for the leukemogenic activity of Trib1.[4] Therefore, we tried to investigate whether the R107L mutation could affect the leukemogenic activity of *TRIB1*.

R107L was introduced into the murine *Trib1* cDNA by site-directed mutagenesis. Both WT and R107L cDNAs were subcloned into the pMYs-IRES-GFP retroviral vector and were used for retrovirus-mediated gene transfer followed by bone marrow transfer according to the method previously described.[1] All the mice

From bloodjournal.hematologylibrary.org at Hirosaki University on March 15, 2012. For personal use only.

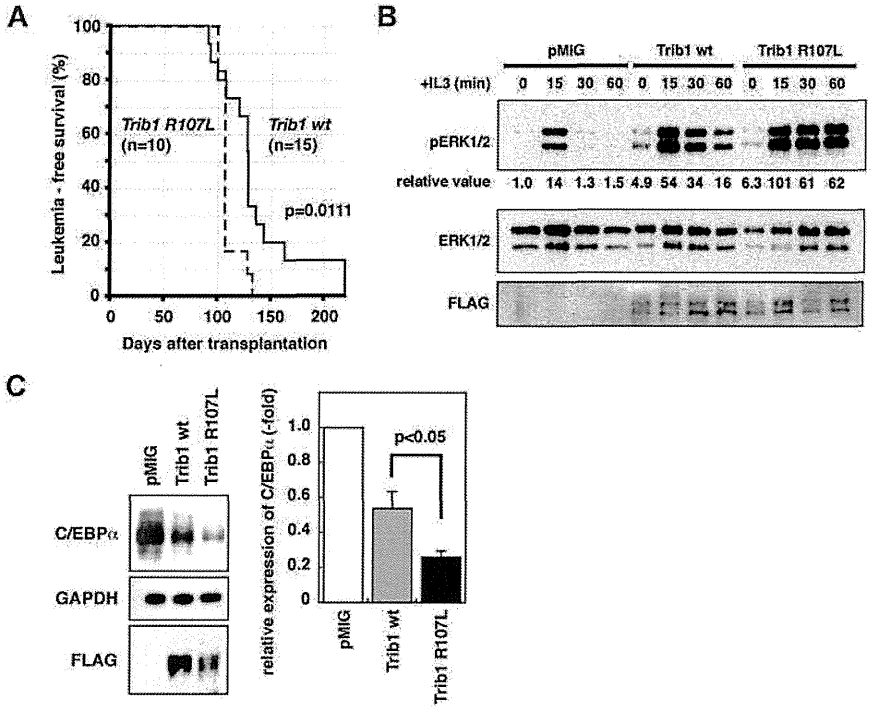

Figure 2. AML development by bone marrow transfer using *Trib1* WT and R107L. (A) Kaplan-Meier survival curves are shown. The *P* value was calculated with the log-rank test. (B) Immunoblot analysis of *Trib1* WT AML (Mac-1 56.2%, Gr-1 52.5%, CD34^{lo}, c-kit^{-}, Sca-1^{-}) and R107L AML (Mac-1 41.4%, Gr-1 25.2%, Cd34^{lo}, c-kit^{lo}, Sca-1^{-}) derived from bone marrow of recipient mice (WT #T73 and R107L #T151 in supplemental Table 1). Enhancement of ERK phosphorylation is more significant in R107L. Relative values of ERK phosphorylation were calculated by densitometric analysis. (C) Immunoblot analysis for C/EBPα of the same AML samples as in panel B. Relative expression level of C/EBPα is quantitated (right).

transplanted with bone marrow cells expressing WT (n = 15) or R107L (n = 12) developed AML (Figure 2A). The mean survival time was shorter in the recipients with R107L-expressing bone marrow cells (110 days) than those with WT (136 days; Figure 2A). The difference was significant ($P = .0111$, log-rank test). The result indicates that the R107L mutation enhances the leukemogenic activity of TRIB1. These results also suggest that *TRIB1* mutation might cooperate with *GATA1* mutation in the genesis of DS-AMKL, and that trisomy 21, *TRIB1*, and *GATA1* mutations occurred consecutively, which contributed to the multistep leukemogenic process.

We have shown that TRIB1 interacts with MEK1 and enhances phosphorylation of ERK.[2] The R107L mutant enhanced ERK phosphorylation more extensively than WT (Figure 2B) in AML cells derived from bone marrow of recipient mice, and more significant degradation of C/EBPα was induced by the R107L mutant (Figure 2C). These findings might be correlated to the enhanced leukemogenic activity of the mutant. Both R107L and WT proteins could interact with MEK1, having the binding motif in their C-termini. The residue 107 is located at subdomain II of the pseudokinase domain.[11] The mutation may affect conformation of the domain and may promote the MEK1 function on ERK, although additional studies are required to address the possibility. A recent study demonstrates that Trib1 and Trib2 failed to show ERK phosphorylation in 32D cells.[12] The different response to Trib1 between primary leukemic cells and the cell line might depend on the cellular context and/or combination of additional mutations. The AML phenotypes were somewhat varied in each case and Mac-1–positive/Gr-1–negative AMLs were more remarkable in WT than in R107L, although the difference was not statistically significant (supplemental Figures 3-4; supplemental Table 1). The current study underscores the role of TRIB1 in human leukemogenesis and the significance of the R107L mutation in its function. Further sequence analysis of tribbles family genes in a larger cohort will emphasize the importance of R107L and/or additional mutations of *TRIB1* in leukemic patients.

Acknowledgments

This work was supported by KAKENHI (Grant-in-Aid for Scientific Research) on Priority Areas Integrative Research Toward the Conquest of Cancer (E.I. and T.N.) and the Ministry of Education, Culture, Sports, Science and Technology of Japan (Young Scientists, T.Y.).

Authorship

Contribution: T.Y., E.I., Y.H., and T.N. designed and performed the research and wrote the manuscript; T. Toki, Y.A., R.K., and M.-j.P. performed the research; and Y.K., T. Takahara, and Y.Y. contributed to the bone marrow transplantation analysis.

Conflict-of-interest disclosure: The authors declare no competing financial interests.

Correspondence: Takuro Nakamura, Division of Carcinogenesis, Cancer Institute, Japanese Foundation for Cancer Research, 3-8-31 Ariake, Koto-ku, Tokyo 135-8550, Japan; e-mail: takuro-ind@umin.net.

References

1. Shimizu R, Engel JD, Yamamoto M. GATA1-related leukaemias. *Nat Rev Cancer.* 2008;8(4):279-287.
2. Jin G, Yamazaki Y, Takuwa M, et al. Trib1 and Evi1 cooperate with Hoxa and Meis1 in myeloid leukemogenesis. *Blood.* 2007;109(9):3998-4005.
3. Kiss-Toth E, Bagstaff SM, Sung HY, et al. Human Tribbles, a protein family controlling mitogen-activated protein kinase cascades. *J Biol Chem.* 2004;279(41):42703-42708.
4. Yokoyama T, Kanno Y, Yamazaki Y, et al. Trib1 links the MEK/ERK pathway in myeloid

From bloodjournal.hematologylibrary.org at Hirosaki University on March 15, 2012. For personal use only.

leukemogenesis. *Blood.* 2010;116(15):2768-2775.

5. Keeshan K, He Y, Wouters BJ, et al. Tribbles homolog 2 inactivates C/EBPalpha and causes acute myelogenous leukemia. *Cancer Cell.* 2006;10(5):401-411.
6. Storlazzi CT, Fioretos T, Surace C, et al. MYC-containing double minutes in hematologic malignancies: evidence in favor of the episome model and exclusion of MYC as the target gene. *Hum Mol Genet.* 2006;15(6):933-942.
7. Kanezaki R, Toki T, Terui K, et al. Down syndrome and GATA1 mutations in transient abnormal myeloproliferative disorder: mutation classes correlate with progression to mye loid leukemia. *Blood.* 2010;116(22):4631-4638.
8. Kogan SC, Ward JM, Anver MR, et al. Bethesda proposal for classification of nonlymphoid hematopoietic neoplasms in mice. *Blood.* 2002;100(1):238-245.
9. Toki T, Kanezaki R, Adachi S, et al. The key role of stem cell factor/KIT signaling in the proliferation of blast cells from Down syndrome-related leukemia. *Leukemia.* 2009;23(1):95-103.
10. Hegedus Z, Czibula A, Kiss-Toth E. Tribbles: a family of kinase-like proteins with potent signaling regulatory function. *Cell Signal.* 2007;19(2):238-250.
11. Yokoyama T, Nakamura T. Tribbles in disease: signaling pathways important for cellular function and neoplastic transformation. *Cancer Sci.* 2011;102(6):1115-1122.
12. Dedhia PH, Keeshan K, Uljon S, et al. Differential ability of Tribbles family members to promote degradation of C/EBPalpha and induce acute myelogenous leukemia. *Blood.* 2010;116(8):1321-1328.

Modern Pathology (2013) 26, 22–31
© 2013 USCAP, Inc All rights reserved 0893-3952/13 $32.00

Duodenal follicular lymphoma lacks AID but expresses BACH2 and has memory B-cell characteristics

Katsuyoshi Takata[1], Yasuharu Sato[1], Naoya Nakamura[2], Mami Tokunaka[2], Yukari Miki[3], Yara Yukie Kikuti[2], Kazuhiko Igarashi[4], Etsuro Ito[5], Hideo Harigae[6], Seiichi Kato[7], Eiko Hayashi[1], Takashi Oka[1], Yoshinobu Hoshii[8], Akira Tari[9], Hiroyuki Okada[10], Abd Alkader Lamia Mohamad[1], Yoshinobu Maeda[11], Mitsune Tanimoto[11], Tomohiro Kinoshita[12] and Tadashi Yoshino[1]

[1]*Department of Pathology, Okayama University Graduate School of Medicine, Dentistry and Pharmaceutical Sciences, Okayama, Japan;* [2]*Department of Pathology, Tokai University School of Medicine, Isehara, Japan;* [3]*Department of Medical Technology, Kagawa Prefectural University of Health Sciences, Takamatsu, Japan;* [4]*Department of Biochemistry, Tohoku University Graduate School of Medicine, Sendai, Japan;* [5]*Department of Pediatrics, Hirosaki University Graduate School of Medicine, Hirosaki, Japan;* [6]*Division of Hematology and Rheumatology, Tohoku University Graduate School of Medicine, Sendai, Japan;* [7]*Department of Pathology and Laboratory Medicine, Nagoya University Hospital, Nagoya, Japan;* [8]*Department of Pathology, Yamaguchi University Graduate School of Medicine, Ube, Japan;* [9]*Division of Gastroenterology, Department of Internal Medicine, Hiroshima Red Cross Hospital and Atomic-Bomb Survivors Hospital, Hiroshima, Japan;* [10]*Department of Endoscopy, Okayama University Hospital, Okayama, Japan;* [11]*Department of Hematology, Oncology and Respiratory Medicine, Okayama University Graduate School of Medicine, Okayama, Japan and* [12]*Department of Hematology and Cell Therapy, Aichi Cancer Center, Nagoya, Japan*

We have reported previously that duodenal follicular lymphoma (FL) is distinct from nodal FL and showed more resemblance to mucosa-associated lymphoid tissue lymphoma, and that FL frequently involved the duodenal second portion. In the present study, we examined duodenal FLs and gastric/colonic FLs to clarify the clinicopathological and immunological differences between the tumor types. We analyzed 8 samples of gastric FL, 17 of duodenal ones, and 5 of colonic/rectal ones, and characterized them by immunohistochemistry, immunogenotyping, and histology. Gastric and colonic FLs presented in submucosal to subserosal areas, whereas duodenal ones presented in the mucosal to submucosal layers. Immunohistochemical analysis revealed that duodenal FLs exhibited the following phenotypes: CD10 (+), B-cell lymphoma 2 (BCL-2) (+), BCL-6 (+), activation-induced cytidine deaminase (AID) (−), BACH2 (+), CD27 (+), MUM-1 (−), Blimp-1 (−), and loose CD21 network (duodenal pattern). Gastric/colonic FLs exhibited the following phenotypes: CD10 (+), BCL-2 (+), BCL-6 (+), AID (+), BACH2 (+), CD27 (−), MUM-1 (−), Blimp-1 (−), and a dense CD21 network (nodal pattern). Expression of AID and CD27 in lymphoma cells and the CD21 network pattern were considerably different between duodenal FLs and gastric/colonic ones. Moreover, *in situ* hybridization revealed that, in the duodenal FLs, BACH2 was expressed at the periphery of the tumor follicle and tumor villi. The number of immunoglobulin heavy-chain variable domains VH4 and VH5 were higher in duodenal follicular lymphomoas than in gastric FLs. The lymphoma cells of duodenal FLs are different from those of gastric/colonic FLs, and duodenal FL is distinct even within the gastrointestinal tract. Somatic hypermutation in immunoglobulin genes and CD27 expression are hallmarks of memory B cells. We suggest that duodenal FL cells are in the memory B-cell stage, and require BACH2 instead of AID for ongoing mutation.
Modern Pathology (2013) **26,** 22–31; doi:10.1038/modpathol.2012.127; published online 17 August 2012

Keywords: BACH2; gastrointestinal follicular lymphoma; memory B cell

Correspondence: Professor T Yoshino, Department of Pathology, Okayama University Graduate School of Medicine, Dentistry and Pharmaceutical Sciences, 2-5-1 Shikata-cho, Kita-ku, Okayama 700-8558, Japan.
E-mail: yoshino@md.okayama-u.ac.jp
Received 25 March 2012; revised 5 June 2012; accepted 6 June 2012; published online 17 August 2012

We have reported that duodenal follicular lymphoma (FL) is a distinct FL by virtue of lacking follicular dendritic cells (FDC), activation-induced cytidine deaminase (AID), and immunoglobulin variable heavy-chain deviation.[1,2] On the other hand, we have also reported that duodenal FLs harbor t(14;18)(*IGH-BCL-2*), exhibit ongoing somatic hypermutations, and express CD10 and B-cell lymphoma 2 (BCL-2), which are common features of nodal FL. However, the proteins have roles in somatic hypermutation in duodenal FL have not yet been identified.

Although the duodenal second portion is the most frequent site of FL in the gastrointestinal tract,[3,4] it sometimes occurs primarily in the gastrointestinal tract outside of the duodenum. Using double-balloon and/or capsule endoscopy, FLs of the gastrointestinal tract primarily involve the duodenum and frequently spread to the small intestine,[3] Few FLs occur in the stomach and colon, but the clinicopathological features of FL in such organs remain unclear. AID has a key role in class switching and somatic hypermutation in B cells,[5] and BACH2 also has a role in these processes in B cells.[6] BACH2 and Bcl-6 suppress Blimp-1, which is a key regulator of plasma-cell differentiation.[7] We have previously reported the lack of AID expression in duodenal FLs, but the entity associated with somatic hypermutation and ongoing mutation remains unknown. Therefore, we focused on BACH2 expression, especially in duodenal FLs, and sought to clarify the differences between duodenal and other gastrointestinal FLs with special reference to the characteristics of FDC, the expression of AID and BACH2, and stage of differentiation in lymphoma cells.

Materials and methods

Patients

Subjects included 8 patients with FL in the stomach, 5 with FL in the colon and rectum, and 17 with FL in the duodenum, which were previously reported.[1] We obtained three samples of reactive lymphoid hyperplasia of the lymph node and three of the duodenum for CD27 immunohistochemical control specimens. Informed consent to use the samples was obtained from all the patients.

Immunohistochemical Analysis

Immunohistochemical staining was performed on sections from 10% buffered formalin-fixed and paraffin-embedded tissues using heat-induced epitope retrieval or trypsin-induced retrieval, an avidin–biotin complex method, and an automated immunostainer (Ventana Medical System, Tuscon, AZ, USA), as previously described.[8] The antibody panel used to assess these cases was as follows (clone, dilution): CD20 (L26, 1:200), CD3 (PS-1, 1:50), CD10 (56C6, 1:50), CD5(4C7, 1:100), Bcl-2 (3.1, 1:200), CD23 (1B12, 1:100), CD27 (137B4, 1:50), and Ki-67 (MIB-1, 1:5000) (Novocastra, Newcastle-upon-Tyne, UK); CD21 (1F8, 1:20), MUM-1 (MUM1p, 1:50) (DAKO Cytomation, Denmark); Bcl-6 (D-8, 1:100) (Santa Cruz Biotechnology, Santa Cruz, CA, USA); cyclin D1 (SP4, ready to use) (Nichirei, Japan); AID (ZA001, 1:100) (Zymed, South San Francisco, CA, USA); and Blimp-1 (3H2-E8, 1:200) (Novus Biologicals, Littleton, CO, USA). Rabbit polyclonal anti-human BACH2 antibody (F69-2) was used as a primary antibody at a dilution of 1:500. Muto *et al*[6] recently reported that staining with the anti-BACH2 antibody was severely diminished in the spleens of BACH2-deficient mice, verifying the specificity of the antibody. For CD20, CD3, CD10, CD5, Cyclin D1, Bcl-2, Bcl-6, and MUM-1 antigens, samples were scored as positive when 30% or more of lymphoma cells were positively stained. For AID expression in tumor follicles, samples with 5% or more expressing cells were scored as positive as previously described.[9] Ki-67-positive cells were counted in tumor follicles. CD21 expression patterns were classified as follows: nodal (>30% positive cells); intermediate (5–30% positive cells); and duodenal (<5% positive cells and FDC located at the periphery of tumor follicles).

Fluorescence In Situ Hybridization (FISH)

FISH for t(14;18)(q32;q21)/*IGH-BCL-2* translocations was performed using the LSI *BCL-2* FISH DNA fusion signal probe (Abbott Molecular, Wiesbaden, Germany) according to the manufacturer's instructions. We performed FISH directly on paraffin-embedded tissue sections and detected the hybridization signal as previously described.[10]

In Situ Hybridization

In situ hybridization was performed on paraffin-embedded tissue sections using a BACH2 RNA probe, which was designed using a modified multi-labeling method as previously described.[11]

DNA Extraction and PCR

DNA was extracted from paraffin-embedded tissue using the QIAmp DNA Micro Kit (Qiagen, Valencia, CA, USA). The variable regions (CDR2 and FW3) and VDJ region (CDR3) of the immunoglobulin heavy-chain (IgVH) gene were amplified by semi-nested PCR, using the primers of FR2, LJH, and VLJH as described earlier.[1,12] Primers used were as follows: 5′-CCGGRAARRGTCTGGAGTGG-3′, as upstream consensus V region primer (FR2); 5′-CTTACCTG AGGAGACGGTGACC-3′, as a consensus J region primer (LJH); 5′-GTGACCAGGTNCCTTGGCCCC-3′, as a consensus J region primer (VLJH). PCR products were purified using the QIAquick PCR purification